Low-Cost Inorganic Solar Cells: From Ink To Printed Device

Susan E. Habas, Heather A. S. Platt, Maikel F. A. M. van Hest, and David S. Ginley*

National Renewable Energy Laboratory, 1617 Cole Boulevard, Golden, Colorado 80401, United States

Received June 21, 2010

Contents

1. Introduction: Low-Cost Photovoltaic Energy

It is increasingly clear that the global reliance on exhaustible natural resources must shift in favor of using sustainable strategies and renewable energy sources in order to provide abundant energy worldwide in an economically viable way. The limited reserves of carbon-based fuels, such as oil, ethanol, natural gas, and coal, along with the environmentally damaging emissions associated with combustion of these fuels, make this transition ever more pressing.[1] However, by 2050, it is predicted that nearly 30 TW (10^{12}) of new power will be needed,[2] which will require dramatic scale changes for noncarbon emitting sources and/or CO_2 sequestration on a global scale. One renewable resource that has the capability to meet the growing energy demand comes in the form of solar radiation, supplying to the earth in one hour an amount of energy roughly equivalent to current annual consumption.[3] While this clean, unlimited source of energy is available, reliable and cost-efficient methods for harvesting it on the terawatt scale pose a tremendous challenge. The direct conversion of solar energy to electricity by photovoltaic technologies represents a rapidly growing component of the electricity market.[4] However, significant cost reductions are necessary to compete with traditionally generated power, and production scaling remains a significant issue.

* To whom correspondence should be addressed. E-mail: david_ginley@nrel.gov.

Susan E. Habas received A.B. degrees in Chemistry and Biochemistry from Wheaton College in Massachusetts in 2001 before joining Professor Peidong Yang's group at the University of California, Berkeley. After attending Massey University in New Zealand as a Fulbright Scholar from 2002 to 2003, she returned to UC Berkeley to study the shape control and selective growth patterns of multimaterial heterostructures for catalytic and energy applications with Professor Yang, leading to a Ph.D. from the Department of Chemistry in 2008. Following a year of postdoctoral research on metal−semiconductor hybrid materials and the fate of nanomaterials in the environment with Dr. Taleb Mokari at the Lawrence Berkeley National Laboratory, she joined the National Renewable Energy Laboratory as a postdoctoral researcher. Her current research interests include the design of functional inks and development of solution deposition processes for photovoltaic materials.

Heather A. S. Platt studied the solution deposition of metal oxide thin films and their conversion to chalcogenides under flowing gas during her Ph.D. work with Professor Douglas Keszler at Oregon State University. She is now developing inks to deposit metal films and lines on silicon wafers for photovoltaic cells as a postdoctoral researcher at the National Renewable Energy Laboratory. Her research interests include identifying new absorber materials for photovoltaics and developing solution deposition processes for electrically active thin films.

10.1021/cr100191d © 2010 American Chemical Society
Published on Web 10/25/2010

Maikel van Hest is currently a Senior Scientist in the Process Technology and Advanced Concepts Group in the National Center for Photovoltaics at the National Renewable Energy Laboratory (NREL). His principal areas of research and expertise include: solution-processing for silicon and thin-film solar cell applications, vacuum deposition, and transparent conductive oxides. His current interests focus on the development and basic science of solution-deposited materials (metals, CIGS, CdTe, and transparent conducting oxides) and the development of next generation process technology for materials and device development (direct-write deposition, spray deposition, and rapid thermal processing). He was the recipient of an R&D 100 award for solution-based CIS solar cells in 2008.

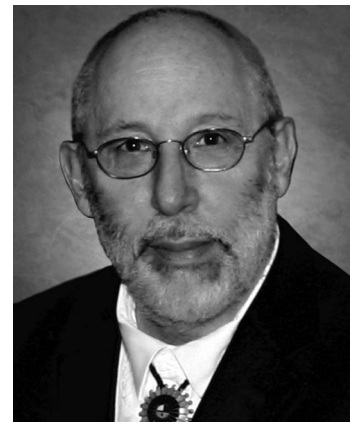

David S. Ginley is a Research Fellow and Group Manager of the Process Technology and Advanced Concepts Group in the National Center for Photovoltaics at the National Renewable Energy Laboratory (NREL). His principal areas of research and expertise focus on the applications of nanotechnology/nanomaterials, organic electronics, transition metal oxides (ferroelectric materials, rechargeable Li batteries, fuel cells, and transparent conductors) and ink jet printing for solar cells. His current work focuses on the development and basic science of very high quality materials (transparent conducting oxides, ferroelectric materials, organic materials, and nanomaterials) and the development of next generation process technology for materials and device development (combinatorial methods, direct-write materials, composite materials, and nonvacuum processing). He received a B.S. degree in Mineral Engineering Chemistry from the Colorado School of Mines in 1972, and a Ph.D. in Inorganic Chemistry from the Massachusetts Institute of Technology in 1976, before joining Sandia National Laboratories from 1976 until 1992, when he joined NREL. He has published more than 400 papers, received 32 patents, and been honored with a Department of Energy Award for Sustained Research in Superconducting Materials, R&D 100 awards for novel chemical etches, for nanoparticle technology, for ferroelectric frequency agile electronics, for alumina based nanofibers, and for solution-based CIS solar cells. He has also received three FLC technology transfer awards, in addition to the Presidents Service Award, which he received in 2007. He is a Professor of Materials Science/Physics at the Colorado School of Mines (CSM) and an Adjunct Professor of Physics at CU Boulder, as well as a member of the Chemistry Department Advisory Board at CSM. He is an Electrochemical Society Fellow, Editor for *Journal of Materials Research* and *Journal of Solar Energy Engineers*, in addition to serving on the Board of Directors for the National Ski Patrol and as the President of the Materials Research Society.

There are a large number of options for solar absorber materials and device architectures, but at this time crystalline and multicrystalline silicon solar cells dominate the market. An emerging class of thin-film devices that is based on amorphous silicon (a-Si), $Cu(In,Ga)Se_{2-x}S_x$ (CIGS), or cadmium telluride (CdTe) is beginning to penetrate the market, making headway in terms of processing costs per unit area.[5] Implementation of thin-film technologies, however, still hinges on the interplay between power conversion efficiency, cost, and reliability. For a material like CIGS that has demonstrated device efficiencies necessary to make it competitive with existing Si-based solar technologies, much of the production cost lies in thin-film deposition. Typically, metal chalcogenide films are deposited by evaporation or sputtering techniques that rely on vacuum environments. The integration of multiple evaporation or sputtering sources provides versatility, leading to control over film composition and the corresponding phase profile but also requires a large capital investment. Furthermore, a considerable amount of energy is required to deposit material from the target sources, and relatively slow throughput and low materials utilization compound difficulties associated with large-scale production using vacuum-based techniques.[6]

Solution-based deposition and processing is an appealing alternative to standard vacuum-based physical vapor deposition (PVD) approaches. The straightforward comparative advantages of solution methods include atmospheric pressure processing, which requires significantly lower capital equipment costs, suitability for large-area and flexible substrates, higher throughput, and the combination of more efficient materials usage and lower temperature processing.[7] In addition, these approaches can be readily adapted for patterning materials, which eliminates the need for subsequent processing steps. The incredible array of solution processing methods that can be applied to photovoltaic device fabrication range from coating processes such as electrochemical and chemical bath deposition, and spin- or spray-coating, to direct-write techniques like inkjet printing, which will be discussed along with the requirements for solution precursors or "inks". Both organic and inorganic materials, as well as their hybrids,[8] are amenable to solution processing methods. Organic materials, more traditionally deposited by solution methods, often have the advantage because their low temperature processability provides an avenue for flexible substrate integration as well as the potential for cost-reduction and minimization of environmental impact.[9] The precedence of inorganic materials comes from their broad spectral absorption, high carrier mobilities, and increased stability. However, the incorporation of many inorganic materials into marketable solar devices is still hampered by efficiency, reliability, and the overall performance metric of price per watt. As ways are sought to make a dramatic impact on the cost of photovoltaic device fabrication, solution-processing approaches come to the forefront in terms of versatility and scalability.

In this review, we will explore the potential of solution processing to lower the cost of conventional Si-solar cell technologies and contribute to the large-scale deployment of thin-film devices. We will cover the development of inorganic solution precursors and corresponding deposition techniques, with the focus on low-cost chemical approaches to semiconductors, conductors, and dielectrics toward an all-solution processed conventional solar cell. Because of the

extensive scope of the subject matter, preference is given to materials and methods that have been directly applied to photovoltaic devices, although every effort is made to direct the reader toward more extensive review articles.

2. Inorganic Photovoltaic Devices

Silicon has long been, and still is, the predominate player in photovoltaic energy conversion, as evidenced by its large share of the solar electricity market. The band gap of Si (1.11 eV) is very close to the optimal value of ~1.3 eV for maximum photoconversion efficiency in a first-generation, single-junction cell.[10,11] However, the indirect band gap and low absorption coefficient require Si thicknesses on the order of 100 μm to adequately absorb the solar spectrum. Consequently, large grain, high-purity Si is needed to minimize carrier recombination, so high temperature purification and crystal growth as well as materials losses during wafer fabrication contribute to the cost of a conventional Si device. Thick film Si on low-cost substrates is of increasing interest but is still in the early stages of development. Second-generation thin-film devices based on CdTe and CIGS absorber layers have the advantage of a direct transition, which leads to a high absorption coefficient and enables the use of much thinner layers (1−5 μm).[12] Furthermore, the band gap of CIGS can be tuned from 1.0 to 2.4 eV by adjusting the atomic ratio of Ga to In, as well as S to Se, allowing precisely graded band gaps.[13] These materials have yielded some of the highest confirmed efficiencies for single-junction polycrystalline thin-film devices to date,[14,15] and, at the same time, are highly amenable to solution processing.

In addition to the absorber material, each component of a solar cell has unique materials requirements, the complexities of which are compounded when considered from the perspective of solution processing. Some parts of a cell are already routinely accessed by solution methods, such as the metal contacts for industrially fabricated crystalline and multicrystalline Si devices that are formed from screen-printed pastes. The driving force for extraction of photogenerated charge carriers from these conventional homojunction devices, depicted in Figure 1a, derives from the built in field at the p−n junction formed by doping the top layer of the wafer (>10^{20} cm^{-3}). Heavy doping at the surface facilitates the formation of an Ag front contact through the antireflection coating (ARC) with a contact resistivity below 10^{-3} Ω cm^2. The back contact contains Al, which provides a back-surface field.[16] A representative heterojunction device, based on CIGS (Figure 1b), typically begins with a 1 μm thick sputtered Mo-back contact on soda-lime glass, followed by the p-type absorber layer (1−2 μm thick) and then a very thin junction layer, also referred to as the buffer. The junction material, CdS (50 nm), is most successfully deposited by a chemical bath technique and is followed by a transparent bilayer of undoped (intrinsic) *i*-ZnO (50−70 nm) that prevents shunting and conductive heavily Al-doped ZnO (120 nm).[17]

Beyond Si, CIGS, and CdTe, there are a large number of materials that have not been thoroughly explored on the sole basis of their lower power conversion efficiencies (PCE). In comparison to the theoretical maximum PCE of 33% for a single-junction cell with a bandgap of ~1.3 eV,[10,11] larger gap materials do not absorb low-energy wavelengths leading to a lower short circuit current (J_{sc}), while smaller band gap materials absorb over a wider region of the solar spectrum, but at the cost of lowering the open circuit voltage (V_{oc}).

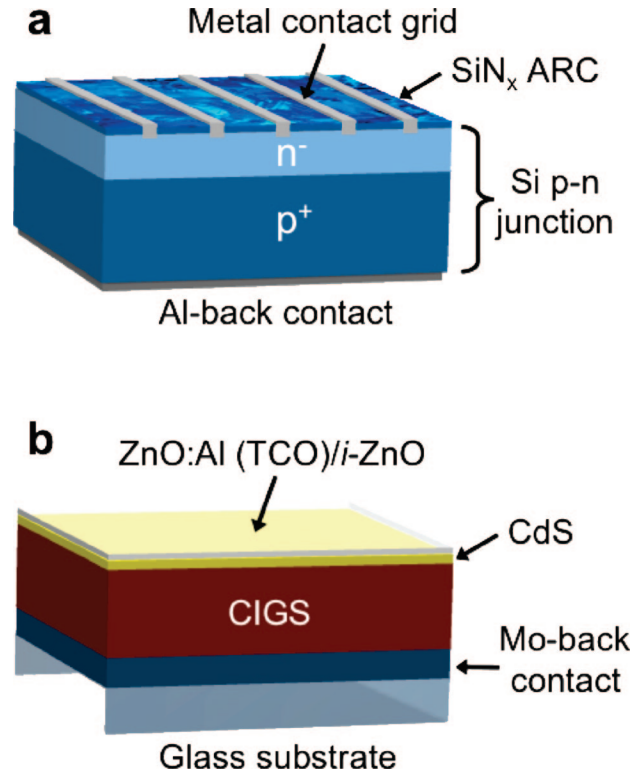

Figure 1. Schematic diagrams of (a) a homojunction Si solar cell and (b) a heterojunction CIGS cell.

However, when extraction costs and supply constraints are considered, a multitude of other absorber materials start to become economically viable if they can be affordably processed.[11] High on the list of new candidates are environmentally "green" and "abundant" materials such as Cu_2ZnSnS_4, which would go a long way toward diminishing concerns about the long-term fate of solar modules. In addition to absorbers, other cost-effective materials including the large band gap semiconductors SnO_2 and ZnO can be integrated as transparent top contacts, and an increasing number of Cd-free buffer materials are under investigation.

It is clear that there is an increasing diversity of inorganic materials emerging for use in new photovoltaic technologies. Although only a few of the processes currently contributing to a finished industrial solar cell are solution-based, the end goal is to access each component of the device, from absorber layer to contact materials, via such processes. In the following sections, we will detail the current state of materials and techniques that advance the objective of a fully solution-processed solar cell.

3. Development of Liquid Precursors

Liquid precursors, both solutions and suspensions, are the key to low-cost thin-film deposition. While capital equipment and operating costs associated with atmospheric processing of liquid precursors are expected to be lower overall than those for vacuum-based techniques,[18] the cost of the ink, depending on the metal species, additives, and solvents used, can quickly become prohibitive. The characteristics of the ink also determine the quality of the final product, the types of substrates that can be used, and requirements for post-processing, all of which can increase the device fabrication costs and limit its application.

Solution-based inks are homogeneous at the molecular level and are often excellent choices for obtaining smooth

layers of uniform composition and phase. In many cases, the precursor stoichiometry can be easily controlled, and there is potential for the facile introduction of dopants.[19] However, solution-based inks are limited by the solubility of the inorganic components, and low weight loading can lead to volume contraction with stress, potential cracking, and delamination upon drying. The solvent and additives as well as conditions such as temperature and pH should be chosen to promote full ink solubility, while at the same time preventing premature precipitation of the final material.

Suspensions containing solid particles prepared by top-down techniques such as ball milling, or bottom-up approaches including spray pyrolysis offer another option for the deposition of normally insoluble materials with high weight loading. The incorporation of nanoscale particles can impart additional advantageous ink characteristics. While nanoparticles have long been used for industrial applications, more recently, a significant degree of synthetic control by solution methods has been realized over a broad range of nanoscale materials.[20−22] For absorber materials, the incorporation of nanoparticles has a number of benefits ranging from physical properties such as tunable electrical and optical characteristics[23] to structural benefits including the arrangement of anisotropic particles to create interdigitated structures with high surface area junctions.[24] Additionally, the reduction in melting point for high surface-area-to-volume materials can promote sintering between the particles under mild conditions.[25,26]

Aside from difficulties filling in void spaces and promoting the growth of large crystal grains, the disadvantages of particle precursors often stem from the organic molecules used for synthetic control and stability. Incomplete removal of the stabilizing agents can result in contamination that can negatively impact the electronic properties of the material and reduce the size of the crystalline domains, which is why vacuum-based deposition techniques have generally demonstrated superior performance over solution coating methods. Achieving effective electrical transport between particles may require additional steps such as annealing or ligand exchange procedures. Even with high temperature treatment, which limits substrate material options, a polycrystalline film composed of sintered nanocrystals can contain a large density of structural defects that lead to limited carrier lifetimes and mobilities.[27] The use of a small volatile ligand or one that decomposes at low temperature, either during synthesis or in a postsynthetic ligand exchange procedure, can minimize residual contamination while instigating contact between particles.

Depending on the method of assembly, closely packed particle arrays can have long-range translational ordering that is absent in randomly oriented polycrystalline solids. Coupling between the quantum dots can promote the formation of artificial quantum dot crystals or nanocrystal solids with three-dimentional minibands arising from splitting of the quantized carrier energy levels in the individual particles.[28,29] Good electronic transport depends heavily on interparticle spacing and the particle surface chemistry, which is influenced by the stabilizing ligands. The large organic molecules commonly used in the synthesis of semiconductor nanocrystals can be exchanged for smaller ligands like hydrazine, amines, or thiols that decrease interparticle spacing and influence the electronic structure.[30−32] Alternatively, these smaller volatile species can be replaced with a more stable molecular metal chalcogenide complex (MCC) such as a $Sn_2S_6^{4-}$ Zintl ion that can act to stabilize nanocrystal arrays and enable strong electronic coupling between neighboring particles or be converted to SnS_2 at only 180 °C to form a composite material (Figure 2).[33] Additional information on this topic can be found in a review by Talapin et al.[34]

Hybrid solution-particle inks that combine solid and dissolved components represent another strategy for producing thin films that leads to an almost unlimited array of material compositions. The solution portion of the ink can be engineered to replace separate organic binding additives, and during processing, the presence of solid particles facilitates the formation of thicker crack-free layers by relieving stress in the film. Additionally, the large contact area between the two phases promotes rapid homogeneous reaction to give the final material.[35] Each ink type, solution, suspension, and dual-phase, has specific formulation requirements to achieve stability and maintain compatibility with the desired deposition and processing techniques to form high-quality films. The primary considerations for ink formulation are the precursor, solvent, and additives, which are chosen with regard to the final chemical composition and phase, deposition and processing techniques, and substrate selection. Ink requirements and formulation guidelines are discussed in reference to inkjet printing[36] and for a number of other coating and printing techniques that will be addressed in the next section.[37]

An ink formulation should be as simple as possible without sacrificing solution stability and final material performance. Once the precursor has been identified, the solvent can be chosen to either dissolve the precursor in the case of soluble ink or to create a particulate suspension. The chemical interaction of the solvent with the precursor determines the loading capacity of the ink. Aqueous solutions are highly desirable because they are cost-effective, and water has no negative environmental impact. On the other hand, organic solvents can be selected to be oxygen free, although carbon-containing solvents have the potential to leave behind other contaminants. There is a tradeoff between volatility and viscosity, with higher molecular weight solvents providing the viscosity necessary for many solution deposition techniques but lacking the volatility required for removal under mild heating. Conversely, solvents with a high vapor pressure can evaporate too quickly and cause nonuniform films or premature precipitation of reactants. In addition to the solvent, a vast selection of additives can be utilized to control the rheological properties and surface tension of the ink. These should be avoided if possible because they are often nonvolatile organic molecules or polymers that remain behind or decompose to form carbon-containing impurities during processing.

The Lewis group has shown that the rheological properties of inks can be precisely tailored for a desired application. In one case, they utilized the loading of poly(acrylic acid) capped Ag nanoparticles to formulate an ink with a shear elastic modulus high enough to form spanning interconnects for a Si solar microcell array, and yet the ink can also be extruded through a 1 μm tapered cylindrical nozzle as a result of the increased shear stress (Figure 3). Annealing printed features at 200 °C for 30 min imparts resistivity values of 5.2×10^{-5} $\Omega \cdot$cm (~30 times bulk), even though full organic removal does not occur until 400 °C.[38]

The selection of substrate and surface treatment is very important because surface energy determines how the ink interacts physically with the substrate,[39,40] and the substrate

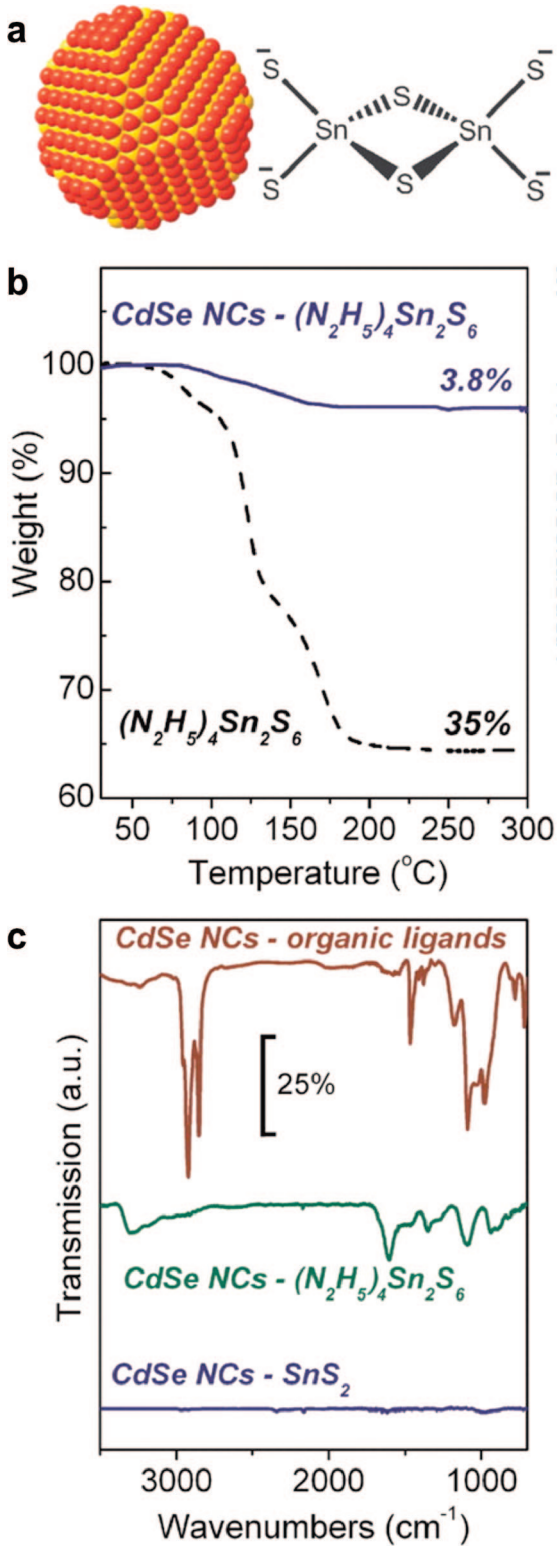

Figure 2. (a) Representation of a CdSe nanocrystal stabilized with $Sn_2S_6^{4-}$ ions. (b) Thermogravimetric analysis of $(N_2H_5)_4Sn_2S_6$ (dashed line) and 3.6 nm CdSe nanocrystals capped with $(N_2H_5)_4Sn_2S_6$ (solid line) showing only 3.8% weight loss upon decomposition of the metal chalcogenide complex (MCC) to SnS_2 below 180 °C. (c) Fourier transform infrared spectra for the CdSe nanocrystals capped with long-chain organic ligands (red trace) and capped with the MCC before (green trace) and after (blue trace) annealing at 180 °C, indicating disappearance of MCC absorption features. Reprinted with permission from ref 33. Copyright 2009 American Association for the Advancement of Science.

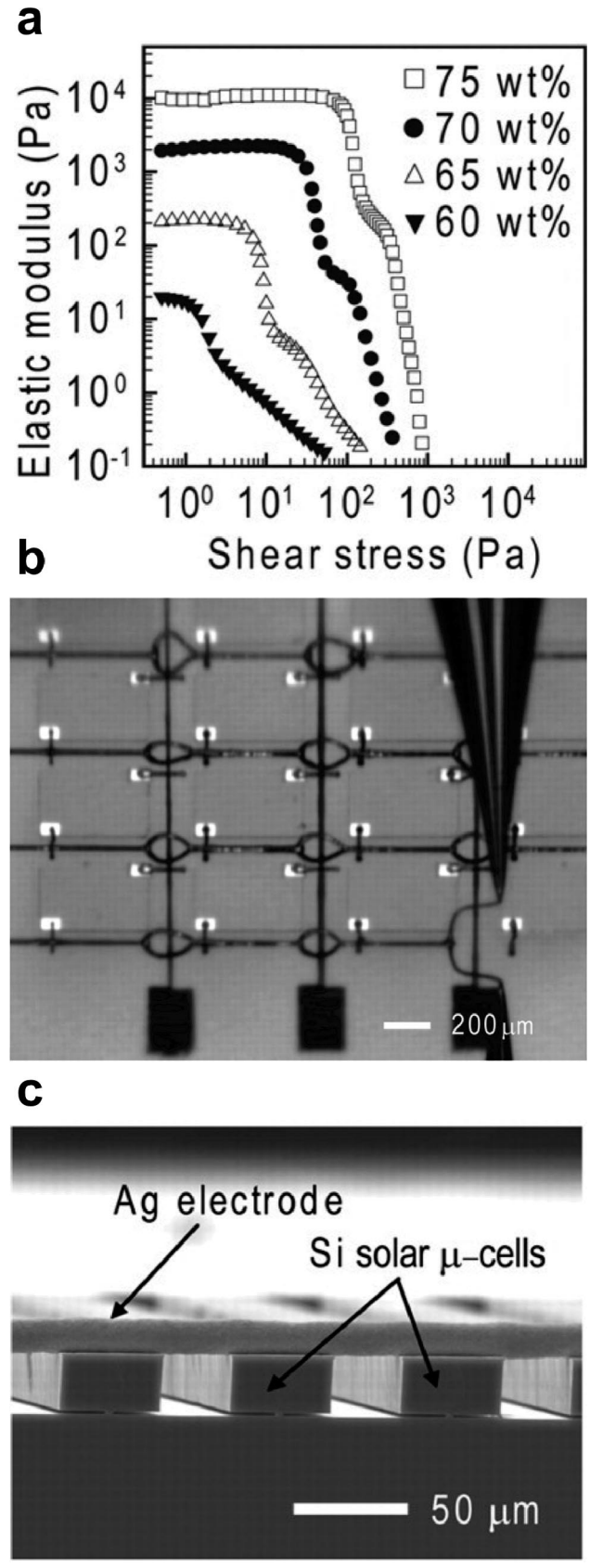

Figure 3. (a) Shear elastic modulus as a function of shear stress for inks with varying Ag nanoparticle loading. (b) Optical image demonstrating the capability of omnidirectional printing to pattern spanning Ag interconnects. (c) Optical image of a Ag microelectrode spanning the unsupported regions of a Si solar microcell array. Reprinted with permission from ref 38. Copyright 2009 American Association for the Advancement of Science.

material places an upper limit on processing temperature. Polymer substrates are cost-effective and flexible, but they are generally not as thermally robust as metal foils or even glass. Polyimide films are one exception, withstanding temperatures to about 400 °C.

Overall, reconciling the complex needs of the ink to meet those inherent to the deposition method is critical for achieving the desired characteristics of the final material. The composition and phase of the material, as well as the film thickness, uniformity, and pattern resolution, all require a carefully balanced combination of precursors, solvent, and additives. Ink formulation for the expanding array of functional materials is still an emerging science. Current progress on ink development for specific solar absorbers, dielectrics, transparent conductors, and metallic conductors will be covered in Section 5.

4. Low-Cost Liquid Deposition Approaches

The development of liquid precursors is intimately joined with the deposition technique, which, by virtue of the engineered ink properties, is capable of meeting the complex demands of uniformity, thickness, resolution, and rate. The application of high-throughput liquid coating and printing technologies is deeply entrenched in existing industries, from newspapers and books to textiles, photography, and ceramics.[37] Increasingly advanced applications are continuously driving the development of not only new functional inks but also progress in deposition techniques, many of which can be applied to photovoltaic device fabrication. For top-side metallization of Si devices, for example, high-resolution lines less than 100 μm in width need to be printed at the rate of one six-inch wafer per second with minimal wafer loss. Screen printing has been traditionally used for this process, but advances in noncontact, direct-write methods such as inkjet and aerosol spray printing are making it possible to achieve a line-width of less than 50 μm on very thin wafers without risking breakage. Coating techniques including ultrasonic spray deposition and slot- or die-coating are useful for uniform large-area coverage to form absorber layers from solution- and nanoparticle-based precursor inks. All of these technologies are scalable for the high-throughput fabrication of photovoltaics from liquid precursors. In the following section, we will review a number of coating and printing techniques that are currently being used or may be applicable for the solution processing of photovoltaics, along with the corresponding ink properties that are suitable for each method.

4.1. Coating Techniques

Strategies for depositing uniform large-area films can be divided into two categories: coating techniques that enable film growth directly on the substrate during deposition, and direct liquid coating methods that require some degree of thermal or chemical treatment to produce the desired composition and phase. Chemical bath, electrochemical, and electroless deposition techniques all fall into the first category. Chemical bath deposition (CBD) is commonly used to deposit a thin junction layer of CdS for $CuInSe_{2-x}S_x$ (CIS) and CIGS devices, which exhibit better performance than those with CdS deposited by chemical vapor deposition (CVD) or physical vapor deposition (PVD). The slow decomposition of thiourea and the subsequent reaction of sulfur ions with cadmium ions released from a Cd salt in alkaline solution provided controlled growth of a high-quality, uniform CdS film on a substrate. The deposition of CdS films and other chalcogenides such as CIS and CIGS, as well as oxide materials, by CBD is a scalable technique that can be utilized for large-area batch processing or continuous roll-to-roll deposition, with only a small investment in capital equipment. The primary drawback comes from the quantity of solution waste associated with this method.[41,42] Closely related to CBD are a number of sequential solution-phase deposition techniques. Rather than including all of the precursors required for film deposition, successive ionic layer adsorption and reaction (SILAR), for example, promotes conformal film growth through repetitive cycles of cation and anion deposition. This process, along with the related electrochemical atomic layer epitaxy (ECALE), have been successfully utilized to deposit chalcogenide and oxide films with controlled thicknesses. Metal films including those of Cu and Ag can be deposited by alternating metal salt deposition with dips in a reducing agent. Much like the gas-phase analogue atomic layer deposition (ALD), sequential solution-phase processes can be time-consuming, particularly with rinsing required between steps, and are more often employed for growing well-defined films with thicknesses on the order of 10 nm.[43] Solution deposition techniques including CBD and SILAR have been reviewed by Bhattachara,[41] and Lindroos and Leskelä,[43] respectively.

Electrodeposition can also be used to create uniform films over large areas, and less waste is generated. Conductive substrates are required for this technique, which makes it suitable for CIS and CIGS film deposition on Mo. A delicate balance of electrochemical and chemical reactions is necessary to achieve the desired film composition and morphology, and high temperature annealing or treatment with additional precursors may be needed.[41] Electroless deposition is an adaptation of electrodeposition, which is carried out by incorporating a chemical component into the bath that is easily oxidized and short-circuiting the conducting substrate to this redox component. Less instrumentation is required for the electroless method, but there is potential for contamination from the additional bath component.[41] Electrodeposition and its electroless counterpart can be used to build up additional metal thickness on printed metal contacts. The metal deposited by these methods can have very high conductivities and forms a good interface with the existing contacts. Light-induced plating (LIP) is also used to build up metal thickness from a chemical bath. This process exploits the photovoltaic effect to induce a negative potential on the front side of an illuminated solar cell.

The benefits of the solution techniques described above include the deposition of high-quality films at atmospheric pressure and room temperature or slightly above, with minimal equipment cost. In addition, solutions can often be recycled, which helps to minimize the waste generated by these processes.

Spray deposition techniques can be used both for the direct growth of films and to deposit liquid inks. In general, an aerosol is formed pneumatically or ultrasonically. In the case of ultrasonic aerosol generation, fine control of a low velocity aerosol can be achieved by varying the ultrasonic frequency, which is inversely proportional to the droplet size. Spray pyrolysis involves the atomization of a liquid precursor that is then directed onto a heated substrate. This method has been extensively reviewed, and when solvent evaporation occurs before contact with the surface, it can be referred to

as spray chemical vapor deposition (CVD).[44] These spray growth methods are ideal for low-viscosity inks, which can be used to grow films that often do not require a subsequent high-temperature annealing step. However, controlled growth in this manner can require longer deposition times than a direct liquid coating approach. Spray deposition can also fall into the category of direct liquid coating, whereby an ink is sprayed onto the surface of a substrate and thermally processed to remove volatiles and byproducts, resulting in the desired composition and phase.

In addition to spraying, there are a number of other low-cost methods for liquid coating precursor inks uniformly onto a substrate, with thermal treatment to remove solvents and additives. These techniques are particularly sensitive to the characteristics of the ink, which can either define the deposition method or be tailored to suit it.

Spin-coating has been used extensively for smaller research scale devices. Ink is deposited onto the substrate, which is then radially accelerated to remove excess ink, leaving behind a uniform layer. Although this technique is not amenable to scaling for in-line production, spin-coating is highly reproducible and suitable for small amounts of ink over a broad range of viscosities. Coating methods that can be used for larger substrates include dip-coating and meniscus coating, which facilitate the deposition of an ink layer by withdrawing the substrate from a reservoir of ink at a constant speed. Whereas dip-coating is most often used when both sides of the substrate need to be covered, meniscus coating can be used to access a single side of the substrate by applying a meniscus of ink to the appropriate side. Depending on the characteristics of the ink and the substrate, patterning, a phenomenon that will be introduced in the next section, can be favored over uniform coverage.

Curtain coating was developed by the photographic industry and takes advantage of highly controlled laminar ink flow. Multiple layers can be deposited simultaneously at very high speeds in excess of 4 m/s by passing a substrate under a curtain of ink. Slide coating is similar to curtain coating, but the laminar ink flow is directed off of a surface that is touching the substrate. Solutions that have been transferred to the substrate surface can be smoothed into a uniform coat by doctor blading, which distributes the ink with a blade or a rod. Either the blade or the substrate can be moved relative to one another, and the thickness of the resulting film is proportional to the gap between the two. Slit casting or die coating is quite similar to doctor blading, except that the ink is delivered by a flow-distribution head through a slit of controlled length and diameter. These methods work better with more viscous inks and can be used for research scale as well as larger in-line production.

4.2. Patterning Techniques

The majority of a single junction-based solar cell is composed of continuous layers, but some of the metal contacts fall in the minority. Light must be able to penetrate the top surface of the device, so metal grids are typically employed to enable this process while still allowing extraction of the resulting photogenerated carriers. Although most of the coating techniques discussed above can be translated for patterning by applying either a physical or a chemical mask, techniques specifically designed to produce high-resolution patterns are simpler and more cost effective. These techniques represent the mainstay of the graphic arts industry, are compatible with roll-to-roll processing, and have more recently been adapted for device fabrication.

Contact methods, where some degree of force is applied to the substrate surface, are more traditionally used for higher viscosity inks. Screen-printing, for example, is similar to doctor blading but with a higher viscosity ink and a physical mask or stencil in place to impart features to the coat. The mask, composed of ink-permeable and impermeable regions, is inserted between the substrate and the blade so that ink is transferred only through the permeable regions to give a two-dimensional pattern with a resolution comparable to that of the mask (50−100 μm).[37] This approach is commonly used to deposit contacts on Si solar cells, for example, although the pressure applied to the substrate requires a minimum wafer thickness. Flexographic printing is a slightly higher resolution method that relies on a raised image on a printing plate cylinder to transfer the pattern to a surface. Flexography has the potential for high-throughput printing and can operate at the high temperatures required for the annealing of functional inks. Even higher resolutions around 25 μm can be achieved with lithographic printing in which hydrophobic and hydrophilic regions of a printing surface produce the positive and negative regions of the image based on the wetting characteristics of the ink. Gravure printing utilizes an engraved metal surface and the transfer of ink from the grooves in the surface to the substrate to give high-resolution patterns (15 μm).[45] All of these methods, however, require a master containing the pattern, making rapid prototyping both difficult and costly.

Noncontact methods, including inkjet, aerosol spray, and laser-transfer printing, enable rapid prototyping as well as the potential for three-dimensional wrap-around contacts, which is incredibly difficult by conventional patterning methods. These direct-write methods also offer maximum ink utilization and scalability to large area manufacturing. Inkjet printing, in particular, is a well-developed technique, and reviews from Schubert and Jabbour highlight its capabilities for patterning functional inks.[46−48] The most common type of inkjet printing applied to functional inks is based on the drop-on-demand (DOD) delivery of a picoliter quantity of ink by piezoelectric actuation. The ink droplet is ejected from the nozzle upon application of the electric field, which creates a pressure pulse in the ink chamber and forces the drop out. When the droplet impinges the substrate, it spreads as a result of momentum and surface tension and then dries through solvent evaporation. An effective process of droplet formation, interaction with the substrate surface, and drying to form the final printed feature requires a high degree of control over the characteristics of the ink and the substrate.[49] When inks for inkjet printing have a low viscosity, in the range of 8−15 cP, and utilize solvents that allow for careful interplay between evaporation in the printhead and on the substrate, printed features less than 20 μm in width are achievable.

More recent advances in direct-write technologies were developed under the DARPA mesoscopic integrated conformal electronics (MICE) program with the goal of creating electronic circuits and materials on any surface.[50] One of the techniques to come out of the MICE program called maskless mesoscale materials deposition uses aerodynamic focusing of a stream of aerosolized ink droplets for the direct writing of patterns with a resolution as low as 10 μm.[51] Theoretical investigation of the forces influencing aerosol spray printing by Schulz and co-workers has led to the

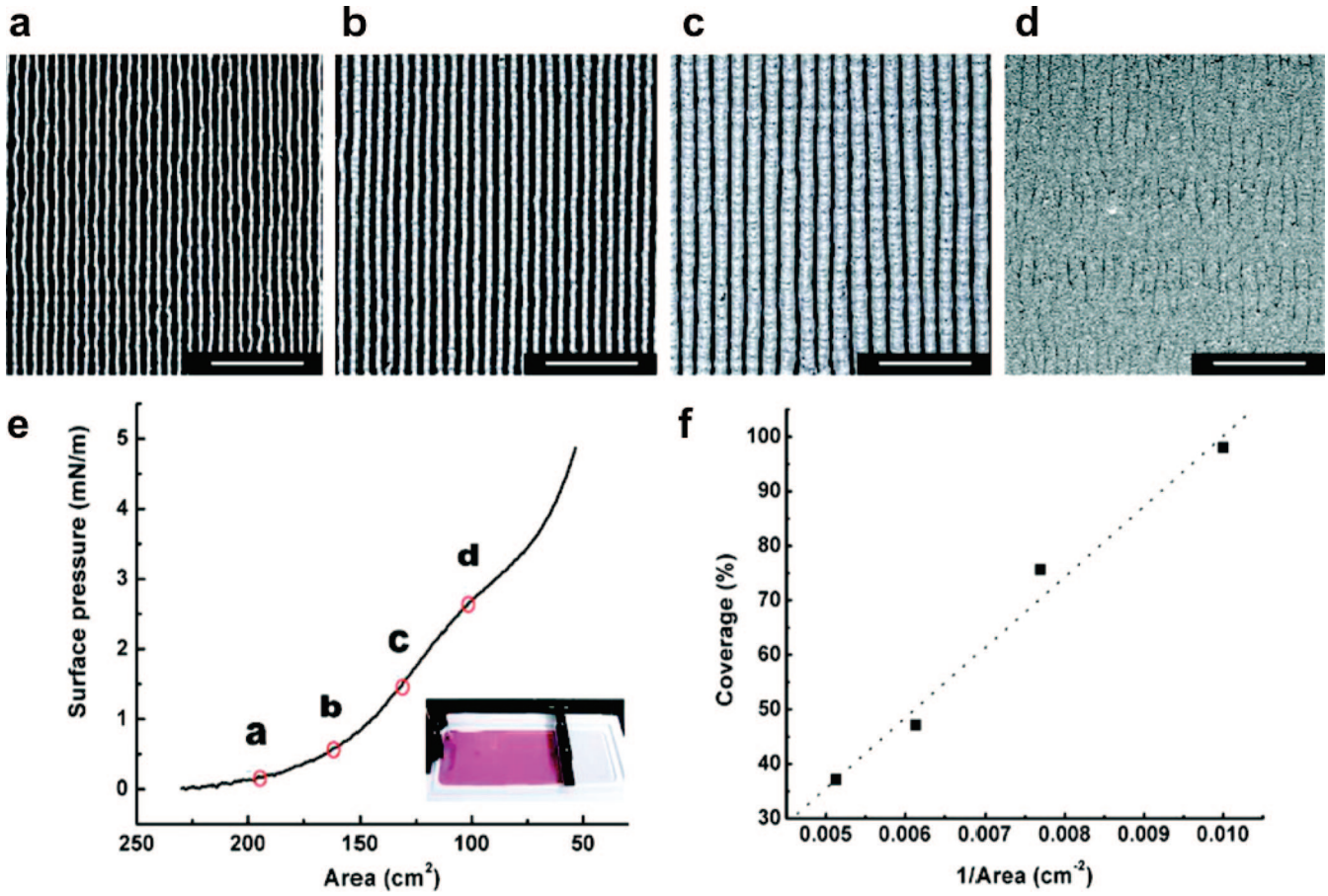

Figure 4. (a−d) Scanning electron microscopy images (scale bars 100 μm) of nanoparticle stripe patterns formed by dewetting of a nanoparticle monolayer onto a substrate during dip-coating. (e) The dimensions of nanoparticle stripe patterns can be tuned by changing the density of the nanoparticle monolayer, (f) leading to a linear dependence. Reprinted with permission from ref 57. Copyright 2005 Nature Publishing Group.

development of a radially varying nozzle system with improved microfluidic control of the collimated aerosol beam (CAB-direct-write technique) that is capable of further narrowing line width to 5 μm.[52,53] The advantages of aerosol-based printing arise from its large processing window. Ink viscosities can range from 1 to 2500 cP, the system is highly tolerant of particulate inks,[54] and high substrate temperatures can be more readily accessed than with inkjet printing, which is more sensitive to solvent evaporation and clogging. The application of aerosol spray printing in photovoltaic device fabrication has been successfully demonstrated at Fraunhoffer ISE for front-side metallizations.[55] Also developed under the MICE program was the matrix assisted pulsed laser evaporation direct-write (MAPLE-DW) technique, a soft version of the laser-induced forward transfer process (LIFT) that relies on the absorption of pulsed UV laser energy by an ink-coated ribbon to induce local solvent evaporation and direct material toward a substrate. In comparison to LIFT, the "soft" nature of the MAPLE-DW approach allows the ink to retain some of the solvent and additives so that it can wet the substrate to give good contact, creating features as fine as 50 μm.[56]

In addition to patterning methods that are dependent on the type of apparatus used, there is an array of techniques that arise from colloidal assembly. As discussed above, in addition to producing a uniform film, dip-coating has the potential to pattern materials based on the characteristics of the substrate and the ink. In this case, the ink is a low-density nanoparticle monolayer that can be transferred onto a substrate by dip-coating. Periodic micrometer-scale metal stripes can be fabricated as a result of fingering instabilities during dewetting at the moving contact line between a hydrophilic substrate and the nanoparticle monolayer (Figure 4). Stripe width increases with surface particle density, while the periodicity of the pattern decreases with faster substrate movement.[57]

This patterning technique and others that depend on dewetting[58] can be used to create metal contact lines with subsequent annealing or seed layers for metal plating. Although these dip-coating techniques are not as high-throughput as some of the other printing techniques, they have the ability to move patterning down into the nanometer regime, along with other colloidal assembly techniques, nanometer stamp printing, and dip-pen lithography.[59−61]

5. Solar Inks

The diversity of inorganic materials that can be deposited by solution methods has expanded dramatically over the past few years. The deposition of thin-film semiconductor layers, transparent conducting oxides, dielectrics, and metals as well as their nanoparticle analogues is becoming routine. Even a material like Si, which historically has not been amenable to solution processing because of its oxidation potential, has gained headway with new synthetic approaches. A primary driving force behind the choice of new materials and precursor chemistries has been the goal of solution-processed photovoltaic devices, which requires large-area deposition of very high quality electronic materials at low cost. A

significant degree of control over the composition, phase, defects, doping, and interfaces is necessary to attain materials that can be integrated into high-efficiency devices. Optimization of this complex array of parameters depends on the precise selection of precursors, solvents, and additives, which also need to be tailored to the deposition and processing techniques. The range of custom designed inks is rapidly evolving and provides tremendous momentum toward a fully solution processed solar cell. In this section, we will review the current progress on ink development for absorber materials, buffer layers, transparent conductors, and metals.

5.1. Thin-Film Absorber Materials

5.1.1. High-Efficiency Materials

Metal chalcogenide semiconductors have played an active role as absorber layers for thin-film photovoltaic devices. Some of the highest confirmed efficiencies for single-junction polycrystalline devices have been achieved with CdTe and CIGS layers.[14,15] The electronic properties of the metal chalcogenide, vital to device performance, are dictated by the elemental composition, crystal phase, grain structure, and density of the film.[17] Solution precursors often have the advantage of easily controlled chemical composition, but formation of the desired crystal phase and the development of large crystalline domains can present a challenge for both solution and nanoparticle inks. A variety of inks have been developed for the solution processing of metal chalcogenide thin films for solar cells. Inks for chalcopyrite materials such as CIS and CIGS have enjoyed particular attention, along with deposition and processing strategies for achieving the desired compounds.[6,62] Although these materials have been recently reviewed by Hibberd et al.[6] and Todorov et al.,[62] they are also discussed here with the intent of highlighting advances in ink formulation along with some more recent results.

5.1.1.1. Copper Indium (Gallium) Sulfide and Selenide. Vacuum-based deposition of CIS and CIGS for high efficiency devices is typically achieved by either coevaporation of the constituent elements or sequential processes employing stacked combinations of metal, chalcogenide, and chalcogen precursors deposited by sputtering or thermal evaporation. The latter technique often relies on thermal treatment of the stacks in a selenium- or sulfur-containing atmosphere to yield the desired composition and crystal phase. A conceptually similar technique can be employed for solution processing of CIS and CIGS films. Metallic alloy films, including those containing Cu and In, have been prepared by annealing a spin-coated film of metal salts in a reducing atmosphere. Subsequent selenization of the resulting metal film in Se vapor yielded devices with efficiencies as high as 9%.[63] The application of metal salts such as chlorides, nitrates, sulfates, acetates, etc., as precursors has been widely studied because of their low cost and high solubility in a broad range of aqueous and organic solvents. Spray pyrolysis of metal−nitrate salt solutions, or spin-coating of sol−gel precursors, gives clean conversion to the corresponding mixed oxides, which can then be annealed in chalcogen vapor to form CIS or CIGS films.[64−66]

Deposition of compositionally homogeneous absorber layers with consistent coverage by liquid coating methods often benefits from a more complex ink containing additives to prevent crystallization of metal salts and improve ink rheology. The addition of ethylcellulose to a solution of metal

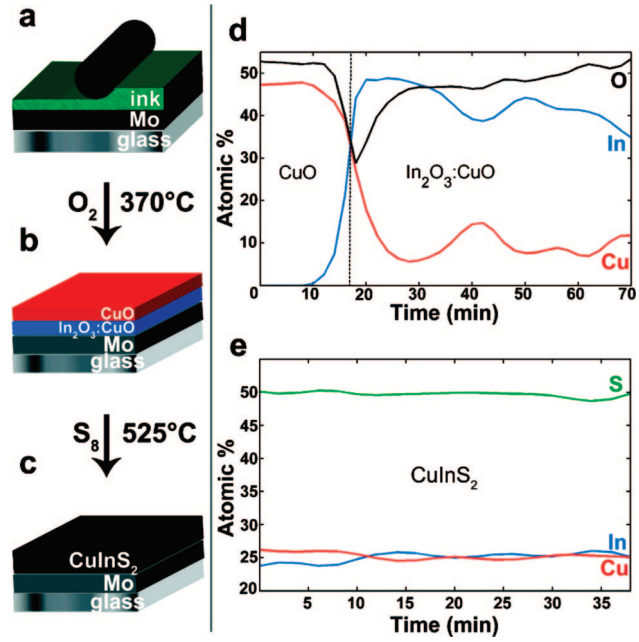

Figure 5. (a) Deposition of vulcanized $CuInS_2$ ink by an air-stable ink rolling process, followed by (b) oxide bilayer formation by heating at 370 °C in air and (c) sulfurization in sulfur vapor at 525 °C. (d) Auger electron spectroscopy depth profile of the bilayer CuO/In_2O_3:CuO film which is carbon-free, and (e) the final $CuInS_2$ film after KCN etching, which is uniform and without impurities. Reprinted with permission from ref 68. Copyright 2010 American Chemical Society.

nitrates afforded an ink of higher viscosity amenable to coating by doctor blading. Following heat treatment at 250 °C in air to remove the cellulose, the film was selenized at 560 °C in a dilute selenium vapor to give CIGS devices with up to 6.7% efficiency.[67] The introduction of carbon containing binders such as ethylcellulose can act to improve the deposition quality of the ink. However, despite the notable efficiencies, a layer of amorphous carbon was observed toward the back contact, indicating that the solvent and/or binder was inadequately removed during heat treatment.[67] Careful interplay between the beneficial effects of additives and their ease of removal is required to produce dense films of sufficient thickness that are compositionally and phase-pure without detrimental impurities. Another approach exploits the vulcanization reaction between S and acetylacetonate salts of copper and indium to make a viscous polymer that can be coated onto a substrate using a roller bar similar to a Mayer rod (Figure 5). The film is heated in air at ∼370 °C to remove the organic material and leave behind air-stable Cu−In oxide that can be converted to $CuInS_2$ by sulfurization in a bomb at 525 °C using elemental sulfur. Although the initial device efficiency reached only 2.15%, no sulfur or carbon residues were detected in the films after annealing in air, indicating successful removal of the ink decomposition/oxidation products.[68]

All of the inks discussed thus far necessitate a secondary sulfurization or selenization step to achieve the final CIS or CIGS phases. The elimination of this additional step in favor of a fully solution-based process would be advantageous from the standpoint of large-scale production costs. Higher material utilization and the lack of toxic chalcogen vapors make S- and Se-containing precursors very appealing. A significant amount of work has been invested in the spray pyrolysis of soluble metal salts with a source of chalcogen incorporated directly into the ink. Chalcogen precursors that have been

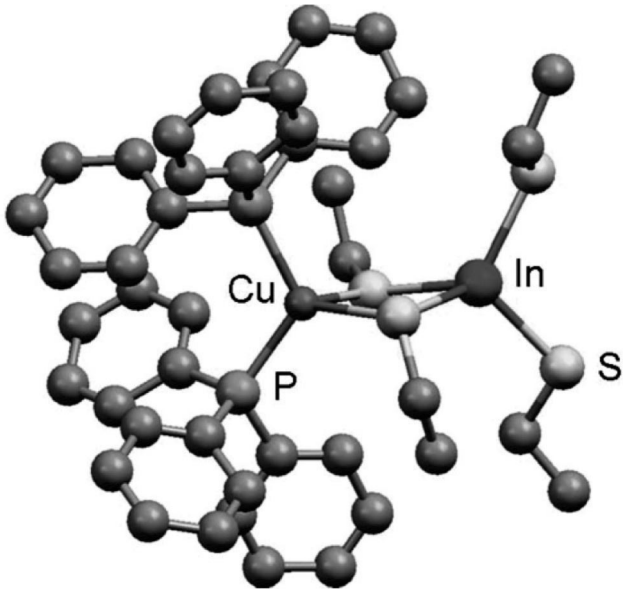

Figure 6. Molecular structure of a single-source $CuInS_2$ precursor, $(PPh_3)_2CuIn(SEt)_4$. Reprinted with permission from ref 76. Copyright 2003 American Chemical Society.

successfully used to deposit variations of CIS and CIGS include thiourea, *N*,*N*-dimethylthiourea, selenourea, *N*,*N*-dimethylselenourea, and thioacetamide, and some of the results from these experiments are included in the cited reviews.[6,69] However, halogen-, carbon-, nitrogen-, and oxygen-containing impurities from the precursors can be difficult to remove at moderate temperatures,[70,71] and annealing in reducing H_2S or a S-containing atmosphere is still beneficial with regards to impurity levels and film morphology.[71,72] Films were also produced by spin-coating soluble metal salts and thiourea in the presence of butylamine and propionic acid, which facilitated the formation of CIS nanocrystal films in situ during heating. These small volatile surface ligands were easily removed under mild conditions (250 °C), promoting sintering of the small nanocrystals, in contrast to other procedures in which nanocrystals prepared prior to deposition required removal of long-chain capping agents or separate ligand exchange procedures. The CdS buffer layer was formed in the same manner, giving nanocrystal-based solar cells with 4% efficiency while eliminating processing steps such as high-temperature sulfurization, a cyanide-bath etch step to correct phase purity and grain size, and chemical-bath CdS deposition.[73]

Although a number of inks have been developed that directly incorporate S- and Se-containing compounds, the corresponding thin films often suffer from phase and morphology issues, as well as contamination without post-treatment in a chalcogen or chalcogenide atmosphere. Selenium-containing inks are also less prevalent because of the expense and toxicity of organo-selenium compounds. Alternatively, soluble metal polychalcogenide species or metal organic decomposition precursors that decompose to form the corresponding metal chalcogenides have been extensively investigated as precursors for CIS and CIGS chalcopyrite films and nanoparticles.[44,74−76] These single-source precursors are frequently stabilized with bulky organic ligands or ions and contain tunable sites within the complex (Figure 6) that can enable control of precursor solubility, decomposition, and final material composition.

Polychalcogenide precursors can also be prepared by simply dissolving In-, Ga-, and Cu-chalcogenide parent compounds with excess chalcogenide in hydrazine (N_2H_4) to form metal-chalcogenide anions stabilized by hydrazinium ($N_2H_5^+$) cations in solution. Mitzi and co-workers have published a number of excellent reviews on this topic.[69,77,78] Hydrazine serves multiple purposes in this capacity: a reducing agent for the excess chalcogen, a volatile solvent for the resulting ionic species, and a weakly coordinating ligand that dissociates at relatively low temperatures. These characteristics have enabled the preparation of highly concentrated precursor solutions that decompose cleanly under mild conditions to give phase-pure CIS and CIGS thin films for devices demonstrating 12.2% and 12.8% photoconversion efficiencies, respectively.[62,79] In addition to direct deposition from hydrazine, precursors have been prepared in hydrazine with a secondary solvent such as ethylenediamine[80,81] or redissolved in a mixed solvent system containing ethanolamine and dimethylsulfoxide.[82] Because of its toxic and potentially explosive properties, decreasing the hydrazine concentration or confining its use to precursor synthesis would make this approach more attractive for large-scale device production.

A rich library of soluble ink chemistries has been developed for CIS- and CIGS-based photovoltaic devices, with significant progress toward reducing the occurrence of impurities in the films. Eliminating the need for high-temperature postdeposition treatment in a Se or S atmosphere or a cyanide bath treatment, while at the same time improving the quality and composition of the films in fewer steps, has yielded devices with efficiencies approaching those of their vacuum-deposited counterparts.[79]

Another approach only touched upon thus far utilizes nanoparticles as the primary ink precursor and is reviewed by Todorov et al.[62] The advances in particulate inks parallel those of solution inks. Briefly, films of metal or metal-oxide particles can be treated with an external S- or Se-containing source to give CIS and CIGS films with photoconversion efficiencies above 10%.[83] The drawbacks of these approaches come from low temperature alloying between the metal particles which can promote phase segregation and the intense reduction often required for nanocrystalline oxide particles.[62]

Nanoparticle-based inks provide the option to fix the final metal-chalcogenide composition from the start. Amorphous CIGS nanoparticles (10−30 nm), for example, were prepared by a metathesis reaction between the metal iodides and Na_2Se. A suspension of the particles in methanol and pyridine was sprayed onto a Mo-coated soda lime glass substrate and thermally processed at 550 °C in Se vapor. Although 4.6% conversion efficiency was achieved, pure CIGS phase formation was found to occur at only 400 °C, impeding the growth of large grains from the porous nanoparticle precursor films. The utility of this method, however, lies in composition control from starting materials to deposited precursor film, all of which contain the same metal ratios.[84] In a different process, phase-pure chalcopyrite CIS nanocrystals were synthesized by heating metal chlorides and Se in oleylamine. Rapid introduction of the selenium precursor at 285 °C supported rapid nucleation and growth of the sphalerite phase, whereas heating all of the reactants at only 130 °C prevented supersaturation, leading to preferential formation of the thermodynamically favored chalcopyrite phase. Annealing in Se vapor promoted facile recrystallization and large grain growth, giving device efficiencies of 3.2%.[85] The conversion efficiency was improved to 4.76% by reducing

the void space in the sintered nanocrystal films by controlled volume expansion (~14.6%) of $Cu(In_{1-x}Ga_x)S_2$ upon exposure to Se vapor.[86] Similarly, chalcopyrite $CuInS_2$, $CuInSe_2$, and CIGS nanocrystal inks were dropcast to form films up to 3 μm thick without annealing to remove organics or treatment with chalcogen vapor, although device efficiencies were limited by high series and low shunt resistances.[87] Significant advances in the direct liquid coating of metal chalcogenide suspensions onto metal foil with rapid thermal processing (RTP) leading to independently confirmed 14% efficient devices have come from Nanosolar.[88]

5.1.1.2. Cadmium Telluride. The potential of CdTe as a cost-effective competitor for Si devices has already been demonstrated, but it has been less extensively studied from the standpoint of solution precursors. Thin-film CdTe absorber layers are generally p-type, with a direct energy gap of 1.45 eV and an absorption coefficient of $>10^5$ for energies greater than the band gap. Devices are fabricated in the superstrate rather than substrate configuration, where a TCO (200 nm), typically doped In_2O_3 or SnO_2, is deposited on glass followed by n-type CdS (100 nm). The p-type CdTe 3−5 μm absorber layer follows, and the solar cell is finished with a metal contact. The device architecture allows illumination through the backside.[89] A number of deposition processes such as sublimation−condensation have been investigated as well as solution processes including electrochemical deposition, spray pyrolysis, and screen printing, which have been reviewed by Bonnet,[89] and more recently as sections within articles by Miles et al.[90,91] Electrodeposition is one of the more common solution techniques,[42] with industrial efforts eventually culminating in 10% efficiency for modules by BP Solar,[92] while spray pyrolysis of $CdCl_2$ was adopted by Golden Photon, leading to 8% efficient modules.[89] Screen printing of a CdTe paste containing $CdCl_2$ as a flux, followed by annealing at 635 °C, produced cell efficiencies close to 9%,[93] and a similar process was used by Matsushita to fabricate 8% efficient modules.[89] To decrease the required annealing temperature for this process, zinc blende CdTe nanoparticles were prepared by the metathasis reaction between CdI_2 and Na_2Te in methanol. Films sprayed in a N_2 atmosphere could be effectively annealed at only 400 °C, with less final carbon contamination relative to nanoparticles capped with long chain stabilizing agents.[94] Commonly, the performance of CdTe thin-film devices is enhanced by treating the CdTe layer with a methanolic solution of $CdCl_2$ followed by annealing at 400 °C in air.[95,96] In the case of solution processed films, chloride ions can be introduced during deposition to improve the crystallinity and electronic properties.[89] Although industrial production of CdTe solar cells by companies such as First Solar are currently focused on nonsolution methods,[97] thin films prepared by solution processing exhibited efficiencies that are nearly comparable to those prepared by gas-phase methods.

5.1.2. Earth-Abundant and Environmentally "Green" Alternatives

Aside from amorphous Si, CdTe and CIGS hold the largest market fraction for thin-film solar cells.[98] However, limitations for the sustained availability of In and Te required for CIGS and CdTe solar cells,[99] as well as restrictions on heavy metal usage, has prompted increased exploration of earth-abundant, environmentally benign absorber materials. Binary absorber-materials that fit these specifications such as pyrite FeS_2, Cu_2S, Cu_2O, and SnS, are typically p-type. This feature is observed when electrons are depleted from the valence band of a semiconductor, and the valence band has significant contributions from the metal ion in a compound. The four binary materials profiled here have one important commonality in that the metal ion is not in its highest oxidation state. FeS_2 pyrite contains Fe^{2+}, Cu_2O, and Cu_2S have Cu^+, and SnS includes Sn^{2+}. In each case, further oxidation of the metal is possible, thus removing electrons from the valence band and creating holes. The resulting p-type character enables these materials to act as one component of the p−n junction required to separate photogenerated carriers, but it also means that a heterojunction with an n-type film will be required to create a working photovoltaic device. Common themes that emerge are the effort required to create such junctions and control the absorber stoichiometry with varying degrees of success.

5.1.2.1. Iron Sulfide. From the perspective of materials availability, pyrite FeS_2 is in a class by itself,[11] and its band gap of 0.95 eV and absorption coefficient of 10^5 cm^{-1} for energies greater than 1.1 eV are also very attractive.[100] The large absorption coefficient is particularly advantageous because only 40 nm of pyrite are required to absorb 90% of incident light.[100] Illuminated devices reported to date are all photoelectrochemical (PEC) in nature and produce mixed results, however. A 10−15 nm layer of pyrite on porous TiO_2 returned only 1% efficiency under AM1 illumination, probably due to carrier generation and recombination at or near the surface of the pyrite.[100] With the electrolyte 4 M HI/0.05 M I_2/2 M CaI_2, a similar PEC measurement produced a slightly higher efficiency of 2.8%.[100] The low reported efficiencies may be due to the fact that high quality thin films of FeS_2 pyrite have been difficult to produce regardless of the deposition method selected. The solution-based approaches investigated include electrodeposition, CBD, and spray pyrolysis.

Reports of electrodeposited Fe and S with pyrite as the ultimate goal all utilized water as the solvent and $Na_2S_2O_3$ as the sulfur source.[101−103] The iron was supplied by the Fe(II) salts $FeCl_2 \cdot 4H_2O$,[101] $(NH_4)_2Fe(SO_4)_2$,[102] or $FeSO_4$,[103] and a wide range of concentrations were investigated. Despite utilizing mole ratios as high as 1 Fe:100 S, all of these processes produced films of 1 Fe:1 S, which is far short of the 1 Fe:2 S required. Pyrite was finally formed from all of these films by postdeposition annealing in sulfur vapor. Unlike the electrodeposition studies, a chemical bath process utilizing nonaqueous solvents produced pyrite directly.[104] Elemental S and $Fe(CO)_5$ were dissolved in xylene, toluene, benzene, or mesitylene to obtain solutions of 1 mol Fe:2 mol S. When these solutions were heated to temperatures between 80 and 165 °C, dark films formed on glass, metal, or plastic substrates. These films were identified as pyrite using X-ray diffraction, X-ray fluorescence, and chemical analysis, although actual elemental ratios were not provided.

Spray pyrolysis of an aqueous solution of thiourea and $FeCl_3$ also produced pyrite without resorting to a postdeposition reaction with S.[105] The ink contained 1 mol Fe:>2 mol S and was sprayed in the presence of S vapor. When the same ink was deposited without the additional S vapor in the chamber, the final films contained 1 Fe:1 S. This result was also observed when $FeCl_2$ was used in the ink instead of $FeCl_3$. In light of these observations, the authors proposed that the first step in the reaction mechanism is the hydrolysis of thiourea to form H_2S. This species in turn reduces Fe^{3+}

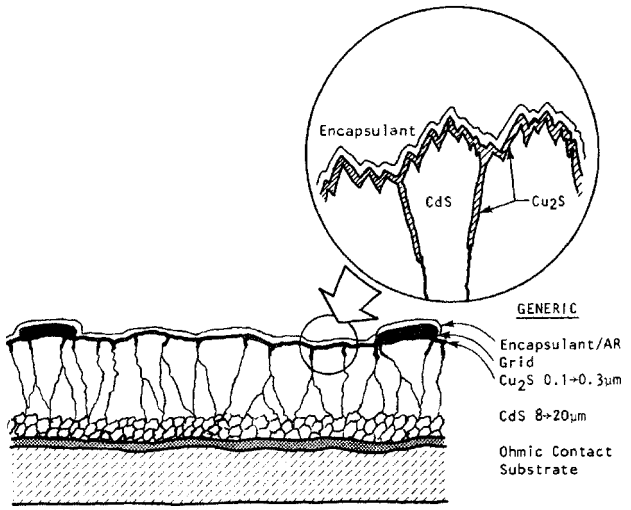

Figure 7. A schematic cross-section of the CdS/Cu_2S thin-film solar cell. Reprinted with permission from ref 110. Copyright 1979 Elsevier BV.

to Fe^{2+}, thus producing polysulfide compounds to react with the Fe^{2+} and additional H_2S to form pyrite. The S vapor introduces additional polysulfides to drive the reaction to completion.[105]

As discussed above, it has been difficult to make pyrite from aqueous solutions. Regardless of the S/Fe ratio in the bath or ink, excess S is required in the vapor phase to successfully synthesize thin films of pyrite. It is very important to control the S concentration carefully because S vacancies have been implicated in the poor device performances reported to date.[106,107] Successful solution deposition of pyrite must include a strategy to form S_2^{2-} in solution, and the use of nonaqueous solvents may help to facilitate this goal.

5.1.2.2. Copper Sulfide. Despite its simple formula, Cu_2S is stoichiometrically and structurally complex. The Cu concentration varies between 1.99 and 2.00 in the chalcocite phase,[108] and if it drops into the range of 1.935 to 1.965, the phase changes to djurleite.[108] Also observed is the phase digenite $Cu_{1.8}S$,[109] thus demonstrating that the Cu stoichiometry of a nominally Cu_2S thin film can vary significantly. Decreasing the Cu concentration has deleterious effects on photovoltaic device performance due to increased carrier concentration, decreased minority carrier lifetimes and mobility, and even changes in the optical absorption.[108] With an indirect band gap of 1.15 eV,[108] the chalcocite phase provides the optimum photovoltaic device performance and the most efficient Cu_2S solar cells.

At better than 9%, the most efficient solar cells utilizing p-type Cu_2S as an absorber also include CdS as the other half of the p−n junction.[108,110] The Cu_2S layer is formed by immersing a CdS film in an aqueous CuCl/NaCl bath where a rapid ion-exchange replaces Cd^{2+} with two Cu^+.[110] A rinse step after the film is removed from the bath washes away any additional $CdCl_2$ on the film.[108,110] The result is a well-defined interface without the adhesion issues that so often plague solution deposited films (Figure 7).

Thin films of Cu_2S deposited by spray pyrolysis have also been integrated into photovoltaic devices, and the conversion efficiencies vary widely.[111] An aqueous solution of CuCl and thiourea combined in a ratio of 1 Cu:3 S was sprayed on a 280 °C substrate.[112] These Cu_2S films were incorporated into solid-state devices with n-type $Cd_xZn_{1-x}S$, and the best result was 7% conversion efficiency when illuminated at 100 mW/cm^2. Another ink utilizing thiourea was prepared by a two-step process.[113] Ethylenediamine (2 mL) was added dropwise to 5 mL of 2 M $CuCl_2 \cdot 2H_2O$ to form a solution containing 1 mol Cu:3 mol ethylenediamine. This solution was dried in air to give a solid, rinsed, dried again, and finally redissolved in ethanol. Enough thiourea was added to reach 1 Cu:3 S, and the ink was sprayed on 330 °C substrates. When these Cu_2S films were deposited on NiO/SnO_2:F coated glass substrates and incorporated into a photoelectrochemical cell with an I^-/I_3^- electrolyte, the efficiencies varied between 0.8 and 1.8% upon 300 W illumination.

Although multiple solar cells utilizing Cu_2S as the absorber have demonstrated promising conversion efficiencies, development of this material has largely ceased because of long-term instability.[109] The Achilles heel of many devices employing Cu-containing compounds is the mobility of the Cu ions. In the case of Cu_2S, this migration changes the properties of the absorber and creates regions of Cu metal at the electrodes and in the bulk of the solar cell.[108] These Cu grains may cause short circuits and decrease or destroy device performance. Thus, although it is possible to fabricate Cu_2S films of appropriate stoichiometry via solution routes, this material has largely been rejected for more promising absorbers.

5.1.2.3. Copper Oxide. Like Cu_2S, Cu_2O is typically p-type in thin-film form, although Cu_2O has a direct band gap of magnitude 2.0 eV.[114,115] Many reported studies synthesized Cu_2O by controlled oxidation of Cu metal films in order to test the material as an absorber for solar cells. The highest efficiency reported for these Schottky barrier devices under AM1 illumination is 1.76%.[114] While Cu_2O thin films are typically p-type, both p- and n-type Cu_2O have been deposited electrochemically.[116] For p-type Cu_2O, an aqueous solution of 0.4 M $CuSO_4$ and either 1.8 or 3 M sodium lactate was utilized, with pH values of 9.0 to 13.0 controlled by addition of NaOH. The bath temperature was varied from 40 to 80 °C. For n-type Cu_2O, the pH of the aqueous solution of 0.01 M copper acetate and 0.1 M sodium acetate was maintained between 5.2 and 6.4 by the addition of acetic acid. This bath was held at 60 °C. Electron density must be added to the Cu^+ in order to form n-type Cu_2O, and this can be accomplished via formation of oxygen vacancies. Such vacancies will eliminate holes, so more oxygen is required to form a p-type material. This strategy underlies the bath choices described above. Higher pH solutions like those utilized for the deposition of p-type Cu_2O will have more hydroxide present, thus minimizing O vacancies. Near a neutral pH, the concentration of hydroxide is lower and more O vacancies form.

In the homojunction devices composed of the p- and n-type Cu_2O layers described above, the best efficiency under AM1 illumination was 0.1%.[116] Despite the poor efficiency, these results are of particular interest because there are not many binary compounds that can be reliably synthesized as both n- and p-type. Heterojunctions between n- and p-type compounds can be difficult to form because of interdiffusion, and this problem can be avoided by using a homojunction.

Electrodeposition has also been utilized to form heterojunctions with Cu_2O.[117] The aqueous solution was composed of 0.10 M $CuSO_4$ and 0.25 M malic acid, and the pH was adjusted to 9.0 with NaOH. The bath temperature was 60 °C. When solar cells were made by depositing p-type Cu_2O from this bath on n-type ZnO, they produced a maximum

efficiency of 0.12% under AM1.5 conditions. Given the larger band gap, it is not surprising that Cu_2O solar cells have produced considerably lower efficiencies than Cu_2S-based devices. At 2.0 eV, the current density that can be generated will be considerably lower than that possible for a band gap of 1.15 eV. A more promising solar cell would position Cu_2O as the top cell absorber in a tandem device.[114]

5.1.2.4. Tin Sulfide. The final binary absorber discussed here is SnS, an indirect band gap semiconductor of magnitude 1.14 eV.[118] Thin-film development has been more recent,[118] and many authors focused on optical and electrical properties instead of integration into solar cells. One reported heterojunction between SnS and CdS produced an efficiency of 0.29% under 100 mW/cm^2 illumination.[118]

In an electrochemical study, SnS was deposited from a S-saturated ethylene glycol bath containing 0.05 M anhydrous $SnCl_2$ and 0.10−0.15 M tartaric acid.[119] What is most striking is the 5 mol Sn:1 mol S in the bath. Not only were SnS films synthesized at room temperature, but SnS_2 films were produced over a temperature range of 70−100 °C. Depending on the electrochemical conditions used, the ratio of Sn:S in the SnS films varied from 1.20 Sn:1.00 S to 1.04 Sn:1.00 S. Auger electron spectroscopy depth profiles showed consistent Sn:S through the entire film. The chemical bath containing $SnCl_2 \cdot 2H_2O$, triethanolamine, thioacetamide, and ammonia with 1 mol Sn:18 mol S in a combination of acetone and distilled water is a more typical route to SnS thin films.[120] The deposition was carried out at 35 °C, and 20 h were required to obtain film thicknesses of 0.50 μm. When these SnS films were incorporated into heterojunction devices, the best efficiency was 0.2%.[121]

Spray pyrolysis routes are of considerably greater interest in progressing toward a fully solution processable inorganic solar cell. One ink utilized for this technique is a solution of 1 mol $SnCl_2$:1 mol diethyl thiourea in a mixture of 3 isopropyl alcohol:1 deionized water.[122] The films formed by spraying this ink on 350 °C substrates contained 1.06 Sn:1.00 S.

To date, photovoltaic devices incorporating SnS all have low efficiencies <1%. The exploration of this semiconductor has been incomplete, however, so it is difficult to determine what factors have thus far limited its performance.

Overall, the binary absorbers pyrite FeS_2, Cu_2S, Cu_2O, and SnS are attractive for many reasons. Not only are they composed of readily available elements, but their solution-based thin-film syntheses require consideration of only two elements. Chemical strategies are much less complex as a result. Unfortunately, all four materials have thus far failed to produce reasonably efficient photovoltaic devices that are stable long-term. Better strategies for solution deposition of these promising absorbers will be required before any of them have the potential to contribute to a fully printable inorganic solar cell.

5.1.2.5. Copper Zinc Tin Sulfide and Selenide. Earth-abundant environmentally benign quaternary absorber materials, on the other hand, have shown a higher degree of success despite their complex nature. Kesterite Cu_2ZnSnS_4 (CZTS) is similar to CIGS in terms of its crystal structure and optical properties. It is a p-type conductor with an optical band gap of 1.5 eV and an absorption coefficient greater than 10^4 cm^{-1}.[123,124] Photovoltaic devices deposited by vacuum methods have already demonstrated device efficiencies of 6.7% and 3.2% for the S and Se analogues, respectively.[124,125] Solution methods for CZTS film deposition have not been as extensively studied as those for CIGS, although devices with efficiencies as high as 3.4%,[126] have been achieved with electrodeposited Cu-Zn-Sn precursors that have been sulfurized in an H_2S[126] or S-containing atmosphere.[127] Films photochemically deposited from metal sulfates and $Na_2S_2O_3$ also benefit from H_2S treatment.[128] Spray pyrolysis of metal chlorides and thiourea has been demonstrated both with sulfurization in H_2S,[129] and without,[130] although, as with CIGS films, it can be difficult to isolate a single phase and prevent oxidation. A sol−gel route to CZTS with H_2S treatment has also been demonstrated, giving a device efficiency of 1.6% for an all-solution processed cell.[131]

Nanocrystals of CZTS have been prepared by high-temperature arrested precipitation in the coordinating solvent, oleylamine. A spray-coated film of the nanoparticles exhibited a photoconversion efficiency of 0.23%, notably without annealing or chemical postprocessing.[132] A similar preparation gave nanocrystals that were dropcast and selenized at 500 °C, leading to 0.8% efficient devices.[133] Nanocrystals were also prepared in ethylene glycol with triethanolamine at 170 °C, although a binder was required to prepare smooth, homogeneous films on glass substrates following annealing in a S-containing atmosphere.[134] In the previous case, the presence of a polymeric binding agent promoted film formation but impeded crystal growth as a result of residual carbon-containing species. As discussed in section 3, the combination of solution and nanoparticle precursors can be effectively formulated to produce the desired ink characteristics necessary for uniform film deposition. The developments in solution processing methods for CZTS are similar to those for CIGS and include the use of a hydrazine-based approach, introduced in section 5.1.1, which was used by Mitzi and co-workers to produce a soluble Cu−Sn chalcogenide precursor. The limited solubility of $ZnSe_{1-x}S_x$ was overcome by taking advantage of the in situ formation of dispersible Zn-chalcogenide particles. The dissolved components in the hybrid slurry acted as the binding medium, allowing for crack-free film deposition without the addition of carbon containing additives. Annealing at 540 °C in the presence and absence of elemental sulfur vapor gave $Cu_2ZnSn(S,Se)_4$ with large grains (1−2.5 μm), shown in Figure 8, leading to device efficiencies as high as 9.6%.[35]

5.1.2.6. Silicon. Of all the thin-film devices discussed thus far, the potential to print highly efficient Si-based solar cells under atmospheric conditions is possibly the most tantalizing. However, such research is still in the very early stages and is complicated by the purity and air sensitivity of precursor materials required. Thin-film Si solar cells are generally produced by vacuum deposition methods using silane as a precursor.[135] The solution-phase analogues are hydrogenated polysilanes, which include linear compounds (Si_nH_{2n+2}) and cyclic versions (Si_nH_{2n}) as well as oligomeric and polymeric forms of hydrogenated silanes. These materials are of interest because they are carbon and oxygen free, but they are also difficult to work with because of their oxygen sensitivity. Alternatively, the synthesis of hydrogen-rich polysilanes protected by organic functional groups can impart solubility or facilitate polymerization, leading to higher-order molecular substructures of crystalline Si.[136] The smaller hydrogenated silicon compounds ($n \geq 3$) are a liquid at room temperature, a useful property for solution deposition, but those with $n <$ 10 have a boiling point below their decomposition threshold temperature (300 °C), leading to evaporation instead of thin-film formation. The polymeric silanes also have low solubil-

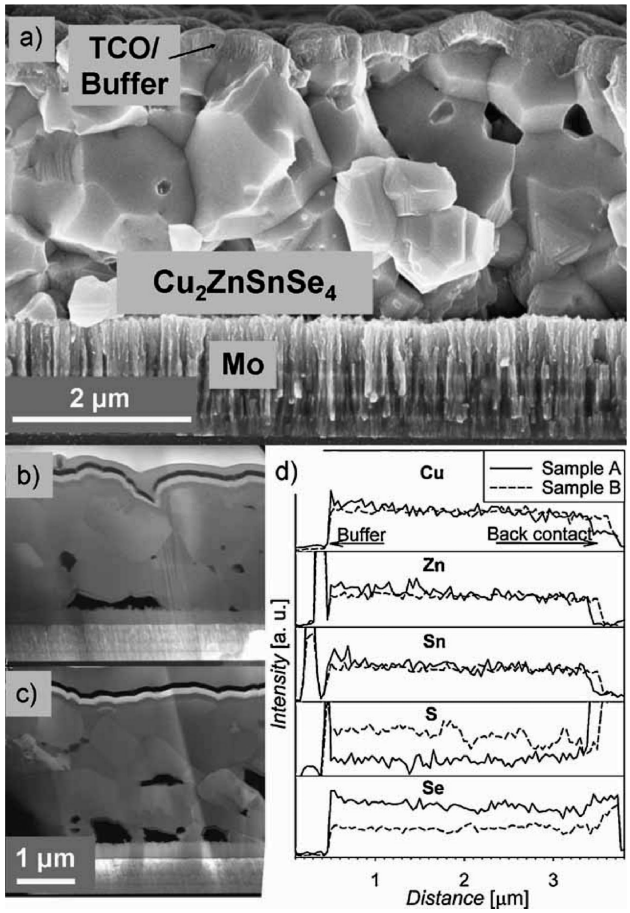

Figure 8. (a) High-performance Se-rich $Cu_2ZnSn(S,Se)_4$/CdS-based device imaged by scanning electron microscopy to illustrate the large 1−2.5 μm grains and isolated voids. Transmission electron microscopy images of (b) Se rich (sample A) and (c) sulfoselenide (sample B) devices with (d) corresponding energy dispersive X-ray spectroscopy profiles showing uniform metal distribution and higher sulfur content in sample B. Reprinted with permission from ref 35. Copyright 2010 John Wiley & Sons, Inc.

ity in organic solvents, which limits their solution processability. Researchers at Seiko Epson and JSR Corporations have found that cyclopentasilane (CPS) that has undergone ring-opening polymerization can be dissolved in a mixture of toluene and CPS to give liquid-Si ink with tunable wetting and coating characteristics.[137] This work has also been reviewed in a book chapter by Furusawa and Tanaka.[138] Spin-coated films of the liquid Si ink were prepared at various temperatures, which controlled the final hydrogen content of the layers. Amorphous Si prepared by conventional CVD contains 5−20% hydrogen,[135] whereas the spin-coated film annealed at 540 °C had only 0.3% hydrogen which contributed to the low observed mobility. The film annealed at 300 °C or below had sufficient hydrogen but were not fully converted to amorphous Si, thus promoting facile oxidation.[137] Crystalline Si films with grains on the order of 10 μm in size are desired for higher mobility materials. Low hydrogen content films were subjected to laser crystallization to produce polycrystalline Si with 300 nm grains as shown in Figure 9, comparable to CVD poly-Si, and mobilities as high as 108 cm^2/V s.[137] Cyclohexasilane was also utilized as a precursor for liquid-Si ink for the fabrication of p−n junction diodes and field effect transistors.[139] Kovio[140] and Innovalight[141] are pursuing Si nanocrystal-based printed inks. Doping of the Si films can be achieved by incorporating

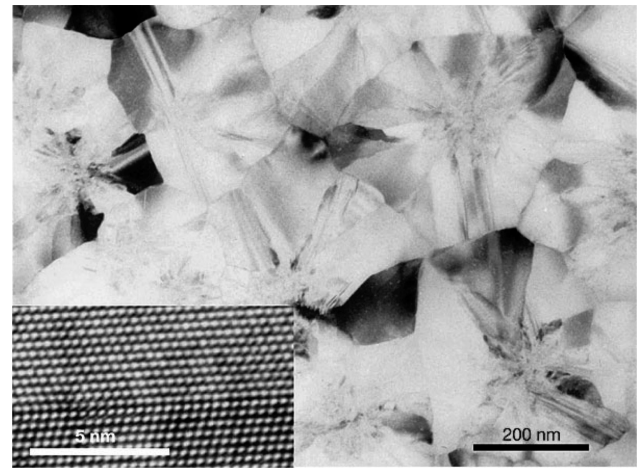

Figure 9. Transmission electron microscopy (TEM) image of a laser crystallized Si thin film prepared from a hydrogenated polysilane liquid precursor. The average grain size of 300 nm is comparable to a conventional chemical vapor deposited film. The high resolution TEM inset highlights the Si lattice structure. Reprinted with permission from ref 137. Copyright 2006 Nature Publishing Group.

white phosphorus (P_4)[142] or an organic boron dopant into the precursor.[139]

5.2. Buffer Materials

Cadmium sulfide (n-type) is most commonly employed as the junction layer for CIS, CIGS, CZTS, and related binary absorber materials as well as CdTe devices.[143] Chemical bath, electrochemical, and electroless deposition methods have been developed for most of the components of a photovoltaic device. However, formation of the buffer layer in particular depends heavily on CBD and has been reviewed by Bhattacharya,[41] although there have been reports of spray deposited and spin-coated layers.[73] As discussed previously, CBD deposition of CdS relies upon the slow decomposition of thiourea and the subsequent reaction of sulfur ions with cadmium ions released from a Cd salt in alkaline solution to facilitate controlled growth of a high-quality, uniform film. The nature of the device architecture necessitates a very thin film with a wide band gap so that light can reach the primary absorber material and photogenerated electrons can be efficiently collected with minimal resistive loss. The high level of control inherent in bath-type methods is crucial for success of the device, which requires a smooth conformal coating to ensure that no short circuits are formed between the TCO contact and the absorber layer. Additionally, CBD acts to remove oxidation products from the film surface[144] as well as facilitate Cd diffusion into the Cu poor CIGS surface layer,[145] or in the case of CdTe, reduce the lattice mismatch. The resulting interface can be very complex but at the same time contributes favorably to device performance.[146] Alternative Cd-free junction materials include Zn(S,Se), ZnO, (Zn,Mg)O, $In(OH)_3$, $In_2(S,Se)_3$, $InZnSe_x$, SnO_2, and SnS_2,[147,148] all of which are potentially amenable to a variety of solution deposition techniques.

5.3. Transparent Conductors

Once the absorber−buffer junction of a photovoltaic device separates photogenerated carriers, they must be extracted via conductive materials. Metals are an obvious choice, but they can prevent light from reaching the absorber.

Alternatively, a transparent conductive material can be used to contact at least one side of the junction, and a large band gap metal oxide is a good choice for minimizing both cost and process complexity. Because oxygen is a necessary component, thin films of oxides can be deposited from the appropriate aqueous solutions in air and, as a result, the majority of the materials cost associated with such films is a function of the metal. To act as an effective top contact for a solar cell, the oxide must have a band gap of at least 3 eV to allow transmission of visible and infrared light. An intrinsic material with such a large gap will be insulating under ambient conditions, so deliberate cation or anion doping is required to move the Fermi level up into the conduction band and produce high conductivity. The intrinsic, insulating oxides are also useful because they provide an additional resistive barrier to short circuits from the transparent conductor through the buffer to the absorber.[143] The lower gap buffer layer can thus be much thinner, which allows more light to penetrate to the absorber to excite carriers.

Solar cells are not the only semiconductor-based devices that require wide band gap materials, and the extensive development of promising oxides for transistors has expanded the knowledge base.[149,150] Of the wide variety of oxides available, the materials ZnO, SnO_2, In_2O_3, and NiO have consistently been successfully integrated into thin-film photovoltaic devices, and they can all be deposited via solution techniques. There are excellent reviews of chemical bath processes that produce all four of these oxides,[151] spray pyrolyzed films of ZnO, SnO_2, and In_2O_3,[152,153] and spin-coated ZnO, SnO_2, and In_2O_3 films.[153] Here we focus on the basic material properties and rationale for utilizing solution deposited ZnO, SnO_2, and In_2O_3, along with typical dopants, and only the most recent thin-film deposition literature will be addressed. Solution deposited NiO thin films will be handled in greater depth because they have not been reviewed recently. Silver nanowire films, a novel nonoxide addition to the transparent conductor family, will also be discussed in more detail.

5.3.1. Intrinsic Oxides

One of the Holy Grails of transparent oxide research has been a p-type material that is truly conductive. Of the four oxides profiled here, only NiO is p-type, while ZnO, SnO_2, and In_2O_3 are all intrinsically n-type. A common feature of the three n-type oxides is that the metal is in its highest common oxidation state: Zn^{2+}, Sn^{4+}, or In^{3+}. As a result, the most likely defect becomes oxygen vacancies, which puts more electron density on the metal and creates excess electrons. In the case of NiO, Ni^{2+} can be further oxidized, depleting electron density from the metal and leaving holes behind.

With an optical band gap of 3.4 eV, ZnO is a transparent compound[149,154] and typical vacuum-deposited films range from 7×10^{-3} to 8×10^{-2} Ω·cm depending on the oxygen partial pressure during deposition.[154] One solution-based ZnO ink was evaluated as the semiconducting layer of a thin-film transistor.[155] Aqueous 2.5 M NaOH (10 mL) was added dropwise to aqueous 0.5 M $Zn(NO_3)_2 \cdot 6H_2O$ (15 mL) to form a zinc hydroxide slurry. After rinsing to remove Na^+ and NO_3^-, the precipitate was redissolved in aqueous NH_3 to obtain a stock solution of 0.14 M Zn. The stock solution was either deposited by spin-coating or diluted with isopropyl alcohol, ammonia, and water for ink jet printing. The ink jet printable ink contained 5.3 M NH_3 and 0.056 M Zn. The spin-coated films and printed lines were ultimately heated on a hot plate in air at temperatures between 150 and 500 °C for 5−10 min to form ZnO. The resulting films were morphologically dense (Figure 10) and performed well in thin-film transistors.

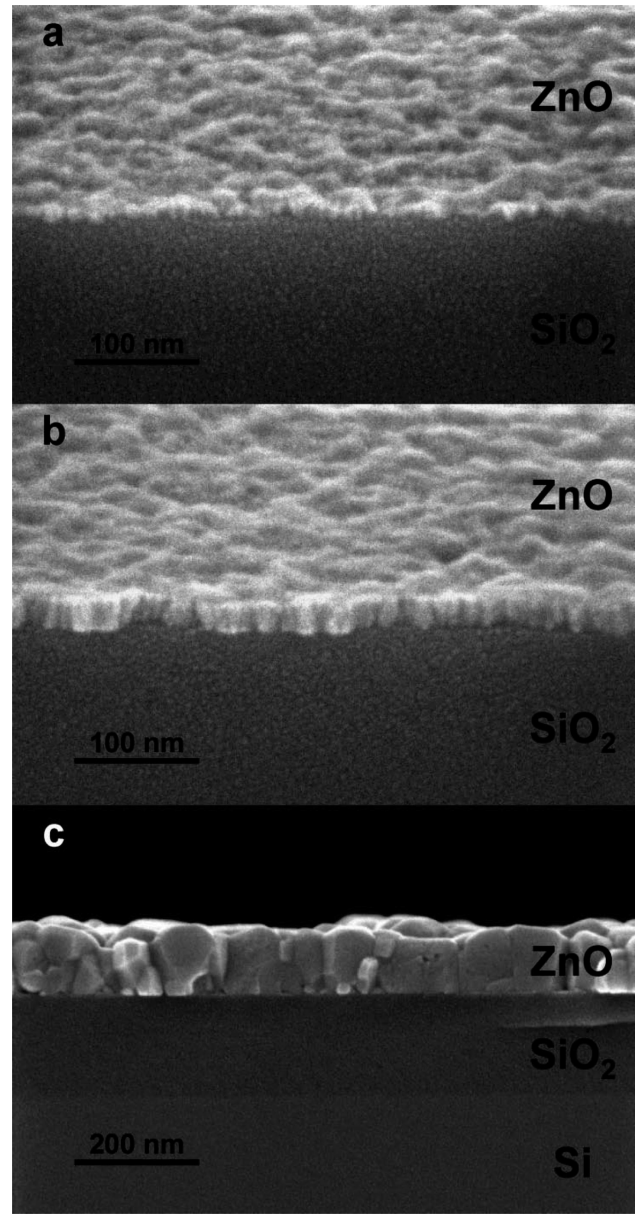

Figure 10. Scanning electron microscopy images of inkjet printed ZnO thin film cross sections (a and b at 45° tilt) annealed at (a) 150 and (b) 300 °C. (c) A spin-coated film annealed to 600 °C in air. Reprinted with permission from ref 155. Copyright 2008 American Chemical Society.

Other solvents have also been used in solutions with $Zn(CH_3COO)_2 \cdot 2H_2O$ as the Zn source. One such ink composed of a 2-methoxyethanol solution of 0.75 M Zn and 0.75 M ethanolamine,[156] was deposited by spin-coating and cured on a hot plate in air at 300 °C for 10 min. These ZnO films were successfully incorporated into solar cells with a poly(3-hexylthiophene) absorber, although the average efficiency of the devices was only 0.09%. A similar ink was also deposited by spin-coating to produce ZnO films of 50 Ω·cm resistivity and 60−95% transmission in the visible region of the electromagnetic spectrum.[157] The most promising large-scale solution-based ZnO deposition was carried

out with an even simpler ink containing 0.02 M $Zn(CH_3COO)_2$ in ethanol, sprayed on a 250 °C substrate.[158] These ZnO films were successfully integrated into CIGS devices to provide quite respectable efficiencies of 12.3%.

While there are reports of a wide range of values,[159] the optical band gap of the best polycrystalline thin films of In_2O_3 is 3.75 eV.[149] These films typically transmit 75−90% of incident visible light,[159] which certainly places them in the transparent realm. Thermally evaporated films have resistivities of 2×10^{-4} to 3×10^{-3} Ω·cm,[160] however, and such values make them too conductive to prevent short circuits to the absorber layer of a stack. As a result, In_2O_3 thin films produced by any method have not found widespread application in inorganic solar cells.

Thin films of SnO_2 are also transparent with a band gap of 3.6 to 4.0 eV,[149,161] and typical resistivities for sputtered films near 1.3×10^{-3} Ω·cm.[162] Tin oxide is the most commonly deposited of the three n-type oxides discussed here[161] because it can be sprayed from a low-cost solution of aqueous $SnCl_4$ on 475 °C substrates to produce films of densely packed, large grain SnO_2.[163] The resistivity of such films is 5×10^{-3} Ω·cm, and they transmit 60−70% of incident visible light. A slight variation utilizes aqueous solutions of Sn(II) chloride along with a substrate temperature of 500 °C.[164] These SnO_2 films transmitted 60−80% of visible light, and their resistivities were 20 Ω·cm. Chemical composition measurements demonstrate that SnO_2 films spray deposited from a chloride salt are always O-deficient and contain some Cl,[159,165] so variation in optical and electrical properties are certainly to be expected.

The nickel-deficient material NiO has an optical band gap of approximately 3.8 eV that has been investigated for electrochromic applications.[166−168] As a result of the nickel-deficiency, some Ni^{3+} forms in addition to the majority Ni^{2+}, and thus NiO has garnered attention from the solar cell community as a p-type transparent contact even though sputtered films have modest resistivities of 1.4×10^{-1} Ω·cm.[169] In organic bulk heterojunction cells, for example, NiO is attractive for its ability to block electrons and readily transport holes,[170] both necessary processes to prevent carrier recombination after photogeneration.

Inks prepared to deposit NiO via chemical bath or spray pyrolysis employ water as the primary solvent. Chemical bath processes have utilized solutions of $NiSO_4$, $K_2S_2O_8$, and NH_4OH[171] or $Ni(NO_3)_2 \cdot 6H_2O$ and urea[172] to deposit amorphous or poorly crystallized $Ni(OH)_2$ or NiOOH films. Postdeposition heating in air produces NiO films that are often porous (Figure 11a), and transmission through these films can be as high as 60−70% in the visible range (400−700 nm). In addition to $Ni(NO_3)_2 \cdot 6H_2O$,[173] the Ni salts $NiCl_2 \cdot 6H_2O$[174,175] and $Ni(CH_3COO)_2 \cdot 4H_2O$[176,177] are employed in solutions for spray pyrolysis. Interestingly, the majority of these salts hydrolyze well enough in water that no additional surfactants or stabilizing agents are required to produce NiO films when the solutions are sprayed on substrates at 330 to 500 °C. One set of films prepared at a substrate temperature of 350 °C from a Ni chloride solution transmitted 80−90% of visible light and had a resistivity of 10^2 Ω·cm.[178] Films prepared from a Ni nitrate solution with LiCl as a dopant were less transparent at 40−60% in the visible range, and photoelectrochemical cells prepared with them had very low conversion efficiencies of 0.3%.

Dip- and spin-coating both rely on controlled hydrolysis of precursor solutions, and the strategy most often pursued

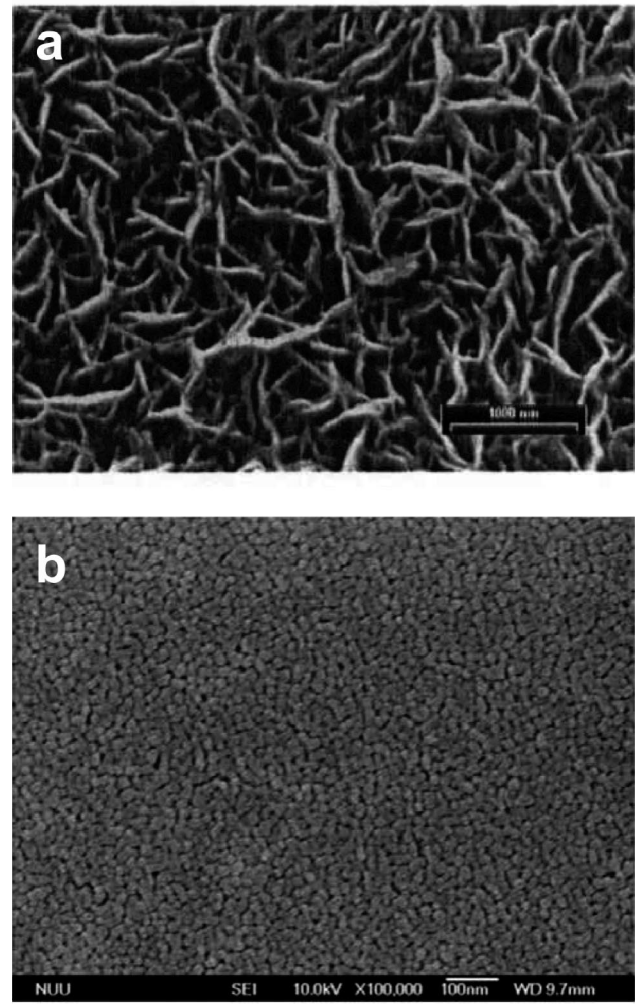

Figure 11. Top-down scanning electron microscopy image of (a) a chemical bath deposited NiO film heated in air at 350 °C for 30 min and (b) a spin-coated NiO film heated in air at 450 °C for 1 h. Reprinted with permission from refs 179 and 180. Copyright 2008 and 2009 Elsevier.

is the use of multiple solvents. When the desired product is a metal oxide, water is an obvious choice that can be incorporated by deliberate addition or by choosing a hydrated metal salt. The nickel salts $Ni(CH_3COO)_2 \cdot 4H_2O$,[180−182] $NiCl_2 \cdot 6H_2O$,[183] and $Ni(HCOO)_2 \cdot 2H_2O$[170] have all been used. Because limiting the availability of water can control hydrolysis, the other solvent is typically an alcohol. Acids or bases can also be used to manage the solution pH, and these species are often chosen because they coordinate the desired metal ion. Amines like ammonia,[180] ethanolamine,[184] and ethylenediamine[170] make frequent appearances in the preparation of NiO films via spin-coating. Film deposition requires heating to drive off solvents and decompose ligands, and then a postdeposition anneal of 250 to 450 °C to crystallize NiO. Transmission through a spin-coated NiO film (Figure 11b) was 60−75% in the visible range, and incorporation of these films into dye-sensitized solar cells gave an efficiency of 0.025%.[180] The performance of a similar NiO film in a bulk heterojunction organic device was much better, with a power conversion efficiency of 3.6%.[170]

5.3.2. Doped Oxides

The ion Sn^{4+} acts as a n-type dopant when it substitutes for In^{3+} in In_2O_3:Sn (ITO) thin films, and sputtered films

have demonstrated resistivities of 3.7×10^{-2} Ω·cm to as low as 6.8×10^{-5} Ω·cm.[160] Increasing the Sn concentration adds carriers and increases the optical band gap, and both of these trends are very useful when high conductivity and transparency are the target properties. Films of ITO are commonly prepared from mixed alcohol/water solutions containing $InCl_3$ and $SnCl_4$.[185,186] These solutions were sprayed on 400−500 °C substrates to form polycrystalline films that transmitted 70−90% of visible light with resistivities of 8×10^{-4} to 1×10^{-2} Ω·cm. In a variation of this method, ITO nanoparticles prepared by spraying aqueous solutions of the chlorides were redispersed in water.[187] Films formed by dipping substrates into this suspension were heated in air at temperatures between 100 and 600 °C. The best films transmitted 90−95% of visible light and had resistivities in the vicinity of 9.5×10^{-2} Ω·cm. Other dip-coated ITO film preparation methods are summarized elsewhere.[160]

Like Sn^{4+} in ITO, Al^{3+} acts as the dopant in ZnO:Al (ZAO). Thin films of ZAO have been prepared by spin-coating alcohol-based solutions of $Zn(CH_3COO)_2 \cdot 2H_2O$, $Al(NO_3)_3 \cdot 2H_2O$, and diethanolamine.[157,188] These films crystallized as ZnO after being heated in the temperature range of 450 to 600 °C, and they have resistivities of 5×10^{-1} Ω·cm and transmit 80−90% of visible light. Aqueous solutions of $ZnCl_2$ and $AlCl_3$ also produce ZAO films when sprayed on 450 °C substrates.[189] Depending on the concentration of Al, these films have resistivities of 2×10^{-3} to 9×10^{-3} Ω·cm, and they transmit 20−80% of visible light. The films deposited from the chloride-based precursor compare very well electrically to vacuum deposited films of ZAO, which had resistivities that varied from 7.0×10^{-3} Ω·cm to 1.4×10^{-4} Ω·cm based on the oxygen partial pressure utilized during the deposition.[154]

The most common dopant for SnO_2 is an anion instead of a cation, and due to its volatility it can only be effectively incorporated into thin films via solution processes. As more F substitutes for O in SnO_2:F (FTO) films, the carrier concentration and band gap both increase.[161] Aqueous, alcohol, or mixed solvent solutions of $SnCl_4 \cdot 5H_2O$ and NH_4F have been sprayed on substrates at 400 to 500 °C to form polycrystalline SnO_2 films.[163,185,190] The higher substrate temperatures produce more transparent films of 75−90% transmission in the visible range,[163,190] while films prepared at lower substrate temperatures transmit 50−75%.[185] The resistivities of the films sprayed at all of these substrate temperatures are in the range of 10^{-3} to 10^{-4} Ω·cm. Another ink that utilized $Sn(CH_3)_2Cl_2$ with NH_4F in aqueous solution was spray deposited in an industrial scale belt furnace.[191] These FTO films had resistivities of 4.1×10^{-4} Ω·cm and transmitted 70−90% of incident visible light. They also performed well in CdTe solar cells, which had very respectable average efficiencies of 14.2%.

5.3.3. Silver Nanowire Films

Ag nanowire films couple the conductivity of a metal with an open structure that also transmits light. If these two attributes were not attractive enough, the open structure also provides enough physical robustness to allow the films to survive bending when they are deposited on flexible substrates.[192] The typical synthetic procedure utilizes $AgNO_3$, polyvinylpyrrolidone, and ethylene glycol to form Ag nanowires of 103 ± 3.7 nm diameter and 8.7 ± 3.7 μm length.[193] Other chemical species like $PdCl_2$[194] or AgCl and KBr[192] can be included to modify the wire diameter and length. After synthesis, suspensions of the wires can be drop cast,[193] sprayed,[194] or spread with a Meyer rod (a small scale technique that approximates slot coating)[192] to form thin films. Drying at room temperature or with moderate heat removes solvent and places the Ag wires in contact with each other in the final randomly oriented array (Figure 12).

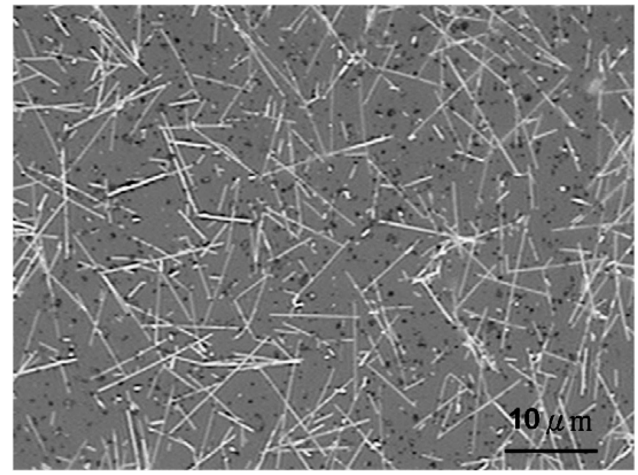

Figure 12. Top-down optical microscope image of an Ag nanowire network on glass. Reprinted with permission from ref 194. Copyright 2010 IOP Publishing.

Table 1. Typical Resistivity and Transmission Values for Solution Deposited Thin Films of Some Important Transparent Conductors[143,157,163,185,187−189,191,195]

material	resistivity (Ω·cm)	max transmission (400−700 nm) (%)
In_2O_3:Sn	10^{-4}	95
SnO_2:F	10^{-4}	90
ZnO:Al	10^{-2}	90

Ag nanowire mesh films have demonstrated visible light transmission up to 80% and sheet resistances ranging from 10 to 100 Ω/sq.[192,193] Unfortunately, no resistivity values have been reported for these films, probably due to the difficulty of accurately estimating the thickness of an open array of wires. In one photovoltaic device incorporating Ag nanowires, the conversion efficiency was only 0.38%.[193] There is clearly room for large improvements in devices using these new transparent conducting films.

As discussed above, both intrinsic and doped oxides play important roles in the top contact of a solar cell. ZnO, SnO_2, and In_2O_3, along with their doped analogues ZAO, FTO, and ITO, have been prepared via solution deposition. The precursors employed are typically simple metal salts in alcohol or aqueous solutions that decompose readily at moderate temperatures. Sprayed ZnO films were successfully integrated into CIGS devices to provide quite respectable efficiencies of 12.3%.[158] The doped compound FTO also performed well in CdTe solar cells, which had even higher efficiencies of 14.2%.[191] The typical resistivity and transmission data for ITO, FTO, and ZAO films in Table 1 demonstrate that all three compounds are good transparent conductors. NiO thin films can also be deposited from simple aqueous Ni(II) salt solutions. The greatest photovoltaic promise of NiO films to date is in the arena of organics, where a bulk heterojunction device incorporating such a film produced a power conversion efficiency of 3.6%.[170] The newest player in the solution deposited transparent conductor game is Ag nanowire composites, which are uniquely poised for integration with flexible low-cost substrates.

Coupled with the appropriate solution deposition techniques, the chemistries described here are promising for large area and high throughput processing of transparent dielectrics and conductors. We conclude that while the intrinsic and doped oxides have all proven their value, the ZnO and SnO_2 based solutions are the best choices because they are composed of earth-abundant elements. Also of particular interest is NiO because it can be incorporated with low-cost, solution-processable organic materials.

5.4. Metal Contact Materials

Metal contact deposition exists as the final link in a completed solar device. For grid-line contacts, reduction of the line width enables a commensurate increase in the active area and consequently in the device efficiency, although higher quality electronic properties are required for size reduction. New ink formulations coupled with deposition and patterning techniques have enabled the production of high quality thin film and grid line contacts over large areas, with electronic properties comparable to their vacuum deposited counterparts. Both solution- and nanoparticle-based inks have experienced considerable advancement,[48] and will be discussed in this section with highlights from recent literature.

5.4.1. Soluble Metal Inks

Early progress on metallization inks for inkjet-patterned photovoltaics focused on metal−organic decomposition (MOD) precursor formulations of copper 2-ethylhexoate, silver neodecanoate, gold amine 2-ethylhexoate, and other variations of metal-carboxylates.[196,197] These metal−organic precursors were often subject to discontinuity upon crystallization, impurities leading to increased resistivity and short-term stability. Nonetheless, inkjet printed tracks of Ag-MOD inks of this type can achieve resistivity values of $2-3 \times 10^{-6}$ Ω·cm, which is about 1.3 to 2 times the resistivity of bulk Ag (1.6×10^{-6} Ω·cm at 20 °C) by thermal processing at or above 150 °C.[40,198] Simple silver salts such as Ag nitrate can undergo thermal reduction to metallic Ag,[199,200] but the high temperatures required for full decomposition are not compatible with many solar devices. Post-treatment in a reducing atmosphere of ethylene glycol vapor for 10 min gives conductive silver tracks at a lower temperature of 250 °C.[201,202]

The addition of a reducing agent directly to the ink is preferable, as it eliminates a secondary step. Strong reducing agents, such as $NaBH_4$, hydrazine, and aldehydes, cause rapid precipitation of metallic silver. Alcohols or amines, on the other hand, can act as reducing agents and in a secondary capacity as stabilizing additives.[203] Low molecular weight solvents and weakly bound additives enable facile removal under mild conditions (150−200 °C). Similar ink formulations, such as Ag trifluoroacetate in ethylene glycol, have been utilized for direct deposition onto a heated substrate, yielding highly conductive lines without postprocessing.[204] Contacts for CIGS photovoltaic cells were inkjet printed at 200 °C on the ZAO layer. A line resistivity of 2.06×10^{-6} Ω·cm and contact resistance of 8.2 mΩ·cm^2 compared to 6.9 mΩ·cm^2 for conventional thermally evaporated Ni/Al contacts were achieved. However, prolonged exposure to the high temperature required for ink decomposition caused some degradation in the conversion efficiency. Still, devices with inkjet printed contacts exhibited 11.4% efficiency in comparison to 11.1% for a reference cell with evaporated contacts that was heated for the same amount of time.[205]

Although the majority of current printed contact work has focused on Ag because of its high conductivity and tolerance to an oxygen-containing atmosphere, inks of other conductive metals are of significant interest as well. Both Ni and Cu represent cost-saving alternatives to Ag, and their low bulk resistivities, 6.9×10^{-6} and 1.7×10^{-6} Ω·cm at 20 °C, respectively, make them desirable targets for ink development.[206−208] An inkjet printable formulation of a Ni-MOD ink, containing a Ni salt and a low molecular weight complexing agent in a reducing solvent, was used to print 80 μm wide lines on a 200 °C glass substrate. The higher resistivity of the printed Ni lines (∼25 times bulk) relative to those deposited from the Ag-MOD ink described earlier is caused by the formation of nickel oxide at high temperature in air.[209] Printed Ni lines, however, can act as an adhesion layer or as a barrier layer to prevent the migration of Cu from the top-contacts into devices. The same Ni-MOD precursor was utilized to deposit a Ni/Ag bilayer by inkjet printing onto finished CIGS devices at 200 °C. The efficiencies of these devices were 11.6% compared to 10.7% for Ag only.[210]

Direct printing of solution MOD inks onto heated substrates has the advantage of eliminating postprocessing steps such as annealing or plating to build line thickness, however, the residence time over the hot surface can degrade the performance of CIGS devices and limit the use of flexible substrates. The use of high-speed printers currently available or under development can minimize the thermal load, but inks that can produce conductive patterns at low temperature or with mild processing conditions are still being actively investigated. Baumann and co-workers showed that UV irradiation enhanced the thermal decomposition of an aqueous MOD precursor to give improved conductivity and decreased sintering time at temperatures as low as 100 °C.[211] Conductive metal patterns could be deposited at room temperature by successively printing an Ag salt and a reducing agent[212] or by using a multicolor inkjet printhead with a separate Cu or Ni salt and a reducing agent.[213] Taking their cue from silver halide photography, Smith and co-workers have printed a common MOD ink, Ag-neodecanoate but then exposed the pattern to UV radiation, followed by development in a solution containing a reducing agent such as hydroquinone. Conversion to conductive metal can be achieved in under a minute at room temperature, and the printed lines were of sufficient thickness to give resistivities as low as 10 times bulk.[214]

5.4.2. Metal Particle Inks

Particle-based metal inks provide another option for mild processing of contacts for solar cells. This technology is somewhat more mature, and Ag nanoparticle inks, in particular, are commercially available for inkjet printing applications.[215,216] The conditions required to form a conductive network between particles in a deposited contact are usually less harsh because decomposition of the precursor is already complete. However, the deposition temperature required for good adhesion to the substrate and conductivity depends strongly on the size of the particles[26] and the organic additives in the ink.[217] Removal of high molecular weight organic capping agents can require high temperature treatment for an extended time to obtain highly conductive lines,[218] and insufficient removal of organic material can

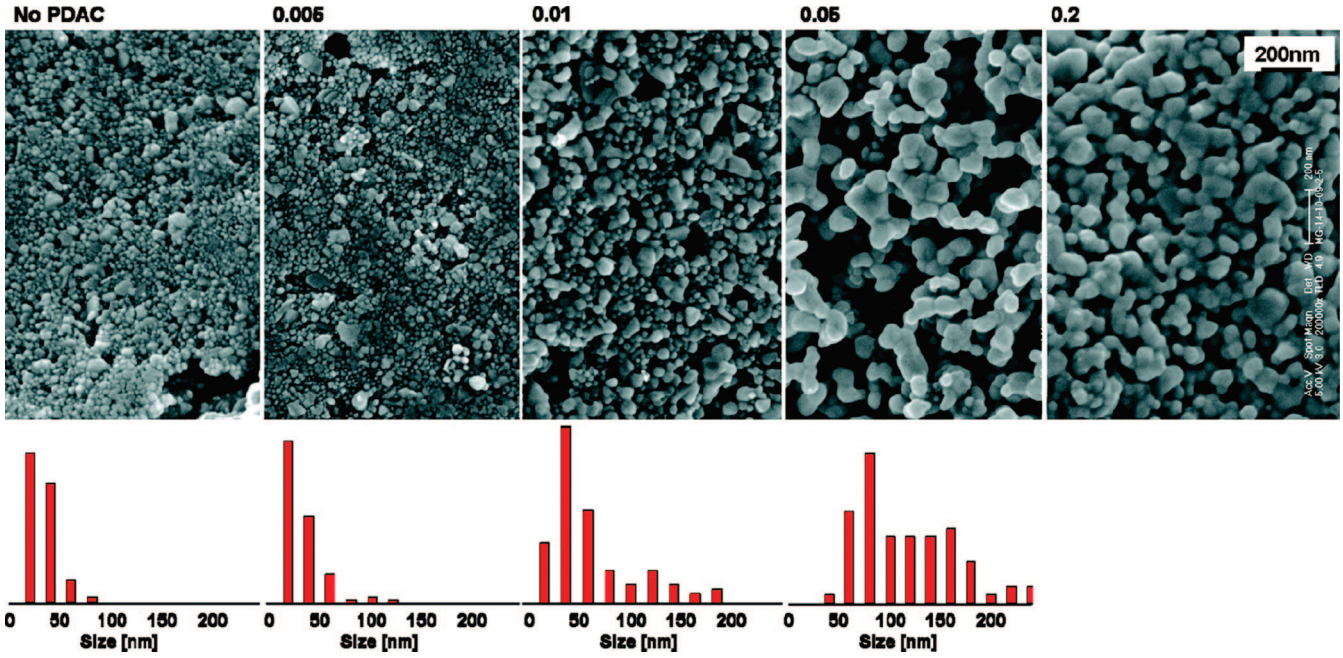

Figure 13. High-resolution scanning electron microscopy images with corresponding particle size distributions for printed patterns of Ag nanoparticles treated with the polycation PDAC at various polymer/Ag weight ratios. Reprinted with permission from ref 224. Copyright 2010 American Chemical Society.

impede grain growth and deteriorate the electrical properties. A number of methods including electrical,[219] laser,[220,221] and microwave[222] annealing, as well as plasma treatment,[223] have been explored to facilitate nanoparticle sintering under mild conditions that are compatible with flexible polymer substrates. A particularly elegant solution to improve the conductivity of printed nanoparticle-based inks has been demonstrated by Magdassi et al.[224] They have found that polyanion stabilized Ag nanoparticles exhibit room temperature coalescence and sintering in the presence of an oppositely charged polyelectrolyte. In solution, Ag nanoparticles stabilized with poly(acrylic acid) (PAA) undergo coagulation in the presence of polydiallyldimethylammonium chloride (PDAC) at concentrations around the point of zero charge. For printed Ag nanoparticle films treated with PDAC (or vice versa), nanoparticle coalescence rather than coagulation begins at a PDAC/Ag weight ratio of 0.01, relative to 0.1 in solution, and leads to a network of large particles at higher weight ratios (Figure 13). Patterns printed by this approach had resistivities as low as 6.8×10^{-6} Ω·cm (5 times bulk).[224] Treatment of Ag nanoparticle patterns with methanol to remove the surface stabilizer (dodecylamine) also resulted in sintering at room temperature, although with higher resistivity.[225]

Silver nanoparticle inks have been the most heavily studied, particularly for inkjet applications,[46,216] but Ni, Cu, and Al nanoparticle inks are as highly sought as their MOD counterparts for their low cost and high conductivities.[226,227] A Cu ink composed of a mixture of nanoparticles and a Cu-MOD precursor was developed with the intention of combining the most desirable traits of nanoparticle and MOD inks. The inclusion of Cu nanoparticles facilitated high metal weight loading, while the Cu-MOD precursor promoted adhesion and sintering of the nanoparticles at a lower temperature. The Cu_2O coating on the Cu nanoparticles was removed by conversion into the same Cu-MOD complex, (hexafluoroacetylacetonato) Cu(I)-vinyltrimethylsilane (Cu(hfa)·VTMS), that was added to the final ink formulation. The hybrid Cu nanoparticle-MOD ink was spray coated in a N_2 atmosphere onto glass and polyimide substrates at 210−230 °C. Films from the hybrid ink had a resistivity of about 2×10^{-3} Ω·cm due to the irregular surface morphology of the film, but the single component Cu(hfa)·VTMS ink achieved a resistivity only an order of magnitude higher than bulk Cu.[228] A similar chelating chemical etching strategy was employed to reduce the oxygen content of Al particle inks.[229,230] The oxidation of Cu nanoparticles can be minimized by controlling the molecular weight of the surface stabilizing polymer,[231] but the introduction of excess organic material can reduce conductivity. Alternatively, air-stable nanoparticle inks composed of Cu with a Ag shell can be prepared by the well-known transmetalation reaction, where the Cu core acts as a reducing agent for Ag ions as a result of the difference in their reduction potentials.[232] While the Cu−Ag core−shell inks are stable in air, annealing inkjet printed patterns in air at 200 °C in air promotes Cu oxidation, although heating under N_2 promotes sintering via Ag migration.[232,233] The same low temperature sintering process was observed for a mixture of Cu and Ag nanoparticles, where the smaller Ag nanoparticles serve to enhance the packing density.[234]

In addition to the standard metallization inks, those that incorporate another component to extend the functionality can provide significant added value to a single processing step. The most common functional component incorporated into metallization inks is a glass frit material that facilitates etching of the dielectric ARC on industrially produced crystalline and multicrystalline Si solar cells. The glass frit, composed primarily of metal oxides, is contained in Ag ink that can be deposited by any number of deposition methods, although screen-printing is generally employed. Rapid thermal processing (firing) at a temperature around 800 °C is required to open the ARC and make contact to the n-type Si emitter layer. The ink used here needs to serve multiple functions: opening the dielectric ARC layer, forming a metal−semiconductor contact with good adhesion, and providing current transport through the contact grid. The requirements of the ink are fairly complex and the process

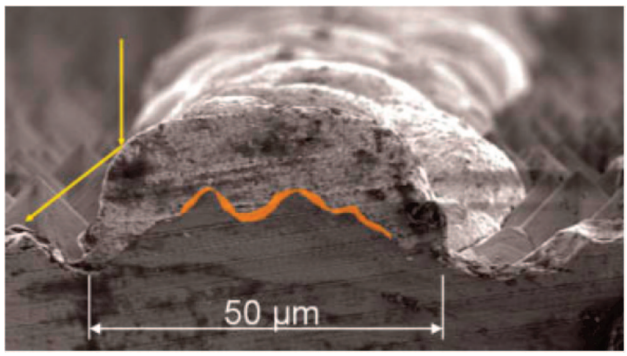

Figure 14. Scanning electron microscopy image showing a cross-section of an aerosol spray printed Ag seed layer containing frit, which was less than 1 μm thick after firing (highlighted in orange). The remaining thickness was deposited by light induced plating of Ag, leading to rounded metal contacts that can promote reflection of incident light (yellow arrows) onto the active solar cell area. Reprinted with permission from ref 240. Copyright 2008 John Wiley & Sons, Ltd.

of contact formation is still not entirely understood, although a number of mechanistic studies on the subject have been published.[235−237] An adaptation on the standard Ag-containing pastes is a hotmelt paste that is a solid at room temperature but can be processed as a conventional paste on a resistively heated screen. The higher Ag content ink solidifies after printing, yielding higher aspect ratio contacts that reduce the line resistivity.[238] Metallization inks containing standard frit as well as those with an alternative frit-replacement have also been deposited by inkjet printing. A two-step process was used to deposit frit-containing ink followed by a pure metallization ink to reduce the amount of Ag required and yield better conductivity.[209,239] In conjunction with a secondary deposition of pure metal which increases line conductivity for lateral current transport, aerosol spray and screen printing of fine-line grids containing frit have been used as a seed-layer to build line thickness of Ag (Figure 14) or Ni by a light induced plating step to give high efficiency solar cells.[55]

Another approach that eliminates the need for high temperature processing and the use of heavy metal containing frit materials involves chemical etching of the dielectric layer. Screen printing of a phosphoric acid-containing etchant paste prior to the Ag paste,[241] or inkjet patterning of a resist layer prior to wet chemical etching,[242,243] have been used. Direct etching of the dielectric layer can be achieved by inkjet printing an aqueous solution of NH_4F, with polyethylene glycol added to reduce the surface tension and increase viscosity, onto the SiO_2 or SiN_x surface coated with an acidic water-soluble polymer such as poly(acrylic acid).[244] The reaction between the printed fluoride ion containing solution and the acidic polymer is similar to the commonly used buffered oxide etching solution, although in this case, the reaction is performed in situ during printing. Following a washing step in deionized water, Ni was deposited by electroless plating to form a good contact, and then line thickness was increased in a Cu plating solution to give 50−60 μm wide contacts and a cell efficiency of 16.4%.[244]

6. Outlook Toward a Fully Printable Inorganic Solar Cell

The development of soluble precursors for thin-film absorber layers, dielectric materials, transparent conductors, and metal contacts, in combination with solution deposition and processing techniques, can be leveraged to prepare fully printed photovoltaic devices. At this juncture, a wide variety of solution coating and patterning techniques are well developed, and noncontact methods such as inkjet, aerosol spray, and laser-transfer printing for high-resolution patterning are emerging with the throughput necessary to compete with conventional methods. The number of materials amenable to solution processing is expanding rapidly, and devices fabricated with solution-deposited absorber materials such as CIGS, CdTe, and CZTS have achieved photovoltaic device efficiencies comparable to those containing vacuum-deposited absorber layers. The less well-studied binary absorber materials show promise, particularly with regards to materials cost and environmental considerations, although pyrite FeS_2, Cu_2O, and SnS thin-film devices are not yet competitive due to issues with film quality, composition, and phase. Devices based on Cu_2S films have provided efficiencies greater than 9%, but they have also demonstrated that significant stability issues must be overcome either through materials development or affordable encapsulation before they could be considered on a larger scale. While certain materials have progressed rapidly within the realm of solution processing, others, including liquid-Si, remain a tantalizing alternative to current wafer-based Si. The propensity of Si to oxidize complicates not only ink development but also subsequent processing. Other semiconductors like CZTS are a challenge because of their inherent complexity. Although the initial results have shown great promise, CZTS is a good example of a complex quaternary system that is not yet well understood. As understanding evolves, a significant degree of control over the ink chemistry and processing will be needed to achieve scalable, low-cost materials with maximum efficiency.

Progress on absorber and buffer materials alone has already provided the potential for fully solution-processed solar cells. These materials, in combination with solution-deposited transparent conductors and metals to extract photogenerated charge carriers, and intrinsic insulating oxides to provide an additional resistive barrier to prevent shunting, are only limited by the quality of the interfaces. Intrinsic and doped oxides, including ZnO, SnO_2, In_2O_3, and NiO, have been successfully deposited by solution techniques for integration into thin-film photovoltaic devices, and ZnO and SnO_2 have the added benefit of an earth-abundant elemental composition. Metal inks and patterning techniques have undergone significant advances in terms of printing resolution for narrow grid-line front contacts as well as low temperature processing of metal−organic and nanoparticle inks to form strongly adhering contacts with conductivities near bulk.

Solution processing of photovoltaic materials has come a long way, and there are demonstrated commercial successes in the areas of metal contacts (screen printing) and transparent conductors (spray pyrolysis). In other areas, the many successful results have been shown on a research level. One of the grand challenges that must be overcome to realize fully solution-processed photovoltaics is to transfer and combine these small scale achievements to the industrial scale at low cost. Effective translation from research to industrial scale will require coordinated advances in materials, interfaces, and processing. The necessary high throughput of large area devices will depend on the rate of coating and printing that can be achieved without compromising the uniformity and resolution of the integrated materials. With reaction kinetics often dictating the rate at which processing can occur, new methods will have to be found to catalyze or otherwise accelerate the rates without introducing impurities. Concurrently, there exists the ultimate goal of reducing

processing temperatures without sacrificing materials quality. Overcoming these considerable challenges will also require a much better understanding of the chemistry of inks and the process by which the precursors react to form individual materials. Moving toward fully solution-processed photovoltaics will rely heavily on understanding and designing the interfacial characteristics of the integrated materials, which will not necessarily behave in the same manner as their vacuum-deposited or otherwise processed counterparts.

Aside from the challenges in these areas, solution processing also offers significant opportunities. Solution processes can facilitate the fabrication of structures that cannot easily be obtained with other methods. Ink-based precursors can be designed to directly produce desired morphologies such as fully dense films or nanoscale arrays. Many opportunities exist for enhancing the performance of existing devices by using nanostructured materials for optical spacers, plasmonics, or nanostructured contacts. The development of third-generation approaches, and the complexity thereof, essentially necessitates the application of solution processing.

Overall, advances in ink chemistry have enabled the deposition of compositionally- and phase-pure materials, which are free of undesirable contaminants that can adversely affect device performance. These same ink formulation strategies can be utilized to tailor the characteristics of the ink to control the interface characteristics. We conclude that the cost-effective materials options, high-throughput deposition techniques, and low-temperature processing schemes reviewed here offer the potential of low-cost solution-processed photovoltaic devices. Such solar cells will tap into the unlimited, renewable solar energy source in order to provide abundant energy worldwide in an economically viable way.

7. References

(1) Holdren, J. P. *Science* **2008**, *319*, 424.
(2) Lewis, N. S.; Nocera, D. G. *Proc. Natl. Acad. Sci. U.S.A.* **2006**, *103*, 15729.
(3) Morton, O. *Nature* **2006**, *443*, 19.
(4) Report of the Basic Energy Sciences Workshop on Solar Energy Utilization, 2005, available online at http://www.er.doe.gov/bes/reports/abstracts.html.
(5) Ginley, D.; Green, M. A.; Collins, R. *MRS Bull.* **2008**, *33*, 355.
(6) Hibberd, C. J.; Chassaing, E.; Liu, W.; Mitzi, D. B.; Lincot, D.; Tiwari, A. N. *Prog. Photovoltaics: Res. Appl.* **2010**, *18*, 434.
(7) van Hest, M. F. A. M.; Ginley, D. S. In *Solution Processing of Inorganic Materials*; Mitzi, D. B., Ed.; John Wiley & Sons, Inc.: Hoboken, 2009.
(8) Milliron, D. J.; Gur, I.; Alivisatos, A. P. *MRS Bull.* **2005**, *30*, 41.
(9) Shaheen, S. E.; Ginley, D. S.; Jabbour, G. E. *MRS Bull.* **2005**, 30.
(10) Shockley, W.; Queisser, H. J. *J. Appl. Phys.* **1961**, *32*, 510.
(11) Wadia, C.; Alivisatos, A. P.; Kammen, D. M. *Environ. Sci. Technol.* **2009**, *43*, 2072.
(12) *Clean Electricity from Photovoltaics*; Archer, M. D., Hill, R., Eds.; Imperial College Press: London, 2001; Vol. 1.
(13) Tarrant, D.; Ermer, J. Conference Record of the 23rd IEEE Photovoltaic Specialists Conference, Louisville, KY, 1993, p 372.
(14) Wu, X.; Keane, J. C.; Dhere, R. G.; Dehart, C.; Albin, D. S.; Duda, A.; Gessert, T. A.; Asher, S.; Levi, D. H.; Sheldon, P. Proceedings of the 17th European Photovoltaic Solar Energy Conference, Munich, Germany, 2001, p 995.
(15) Repins, I.; Contreras, M. A.; Egaas, B.; Dehart, C.; Scharf, J.; Perkins, C. L.; To, B.; Noufi, R. *Prog. Photovoltaics: Res. Appl.* **2008**, *16*, 235.
(16) Poortmans, J.; Nijs, J.; Mertens, R. In *Clean Electricity from Photovoltaics*; Archer, M. D., Hill, R., Eds.; Imperial College Press: London, 2001.
(17) Rau, U.; Schock, H. W. In *Clean Electricity from Photovoltaics*; Archer, M. D., Hill, R., Eds.; Imperial College Press: London, 2001.
(18) Zweibel, K. *Sol. Energy Mater. Sol. Cells* **1999**, *59*, 1.
(19) Yuan, M.; Mitzi, D. B.; Liu, W.; Kellock, A. J.; Chey, S. J.; Deline, V. R. *Chem. Mater.* **2009**, *22*, 285.
(20) Murray, C. B.; Kagan, C. R.; Bawendi, M. G. *Annu. Rev. Mater. Sci.* **2000**, *30*, 545.
(21) Yin, Y.; Alivisatos, A. P. *Nature* **2005**, *437*, 664.
(22) Tao, A. R.; Habas, S.; Yang, P. *Small* **2008**, *4*, 310.
(23) Alivisatos, A. P. *J. Phys. Chem.* **1996**, *100*, 13226.
(24) Gur, I.; Fromer, N. A.; Chen, C.-P.; Kanaras, A. G.; Alivisatos, A. P. *Nano Lett.* **2006**, *7*, 409.
(25) Goldstein, A. N.; Echer, C. M.; Alivisatos, A. P. *Science* **1992**, *256*, 1425.
(26) Buffat, P.; Borel, J. P. *Phys. Rev. A* **1976**, *13*, 2287.
(27) Ridley, B. A.; Nivi, B.; Jacobson, J. M. *Science* **1999**, *286*, 746.
(28) Lazarenkova, O. L.; Balandin, A. A. *J. Appl. Phys.* **2001**, *89*, 5509.
(29) Jiang, C.-W.; Green, M. A. *J. Appl. Phys.* **2006**, *99*, 114902.
(30) Yu, D.; Wang, C.; Guyot-Sionnest, P. *Science* **2003**, *300*, 1277.
(31) Talapin, D. V.; Murray, C. B. *Science* **2005**, *310*, 86.
(32) Law, M.; Luther, J. M.; Song, Q.; Hughes, B. K.; Perkins, C. L.; Nozik, A. J. *J. Am. Chem. Soc.* **2008**, *130*, 5974.
(33) Kovalenko, M. V.; Scheele, M.; Talapin, D. V. *Science* **2009**, *324*, 1417.
(34) Talapin, D. V.; Lee, J.-S.; Kovalenko, M. V.; Shevchenko, E. V. *Chem. Rev.* **2009**, *110*, 389.
(35) Todorov, T. K.; Reuter, K. B.; Mitzi, D. B. *Adv. Mater.* **2010**, *22*, E156.
(36) Magdassi, S. In *The Chemistry of Inkjet Inks*; Magdassi, S., Ed.; World Scientific Publishing Co. Pte. Ltd.: Hackensack, NJ, 2010.
(37) Tracton, A. A. *Coatings Technology Handbook*; 3rd ed.; CRC Press: Boca Raton, FL, 2006.
(38) Ahn, B. Y.; Duoss, E. B.; Motala, M. J.; Guo, X.; Park, S.-I.; Xiong, Y.; Yoon, J.; Nuzzo, R. G.; Rogers, J. A.; Lewis, J. A. *Science* **2009**, *323*, 1590.
(39) Duineveld, P. C. *J. Fluid Mech.* **2003**, *477*, 175.
(40) Smith, P.; Shin, D. Y.; Stringer, J.; Derby, B.; Reis, N. *J. Mater. Sci.* **2006**, *41*, 4153.
(41) Bhattacharya, R. In *Solution Processing of Inorganic Materials*; Mitzi, D. B., Ed.; John Wiley & Sons, Inc.: Hoboken, NJ, 2009.
(42) Dharmadasa, I. M.; Haigh, J. *J. Electrochem. Soc.* **2006**, *153*, G47.
(43) Lindroos, S.; Leskelä, M. In *Solution Processing of Inorganic Materials*; Mitzi, D. B., Ed.; John Wiley & Sons, Inc.: Hoboken, NJ, 2009.
(44) Hepp, A. F.; Banger, K. K.; Jin, M. H.-C.; Harris, J. D.; Mcnatt, J. S.; Dickman, J. E. In *Solution Processing of Inorganic Materials*; Mitzi, D. B., Ed.; John Wiley & Sons, Inc.: Hoboken, NJ, 2009.
(45) Brazis, P. W.; Gamota, D.; Zhang, J.; Szczech, J. In *Solution Processing of Inorganic Materials*; Mitzi, D. B., Ed.; John Wiley & Sons, Inc.: Hoboken, NJ, 2009.
(46) Tekin, E.; Smith, P. J.; Schubert, U. S. *Soft Matter* **2008**, *4*, 703.
(47) Singh, M.; Haverinen, H. M.; Dhagat, P.; Jabbour, G. E. *Adv. Mater.* **2010**, *22*, 673.
(48) Perelaer, J.; Smith, P. J.; Mager, D.; Soltman, D.; Volkman, S. K.; Subramanian, V.; Korvink, J. G.; Schubert, U. S. *J. Mater. Chem.* **2010**, *20*, 8446.
(49) *The Chemistry of Inkjet Inks*; Magdassi, S., Ed.; World Scientific Publishing Co. Pte. Ltd.: Hackensack, NJ, 2010.
(50) Mesoscopic Integrated Conformal Electronics; available online at http://www.darpa.mil/dso/archives/mice/index.htm.
(51) Renn, M. J.; King, B. H.; Essien, M.; Hunter, L. J. U.S. Patent 7,045,015, 2006.
(52) Akhatov, I.; Hoey, J.; Swenson, O.; Schulz, D. *Microfluid. Nanofluid.* **2008**, *5*, 215.
(53) Schulz, D. L.; Hoey, J. M.; Thompson, D.; Swenson, O. F.; Han, S.; Lovaasen, J.; Dai, X.; Braun, C.; Keller, K.; Akhatov, I. S. Proceedings of the Academic Track of the 2008 Flexible Electronics and Displays Conference and Exhibition, Phoenix, AZ, 2008.
(54) Hörteis, M.; Mette, A.; Richter, P.; Fidorra, F.; Glunz, S. Proceedings of the 22nd European Photovoltaic Solar Energy Conference, Milan, Italy, 2007, p 1039.
(55) Mette, A.; Richter, P. L.; Hörteis, M.; Glunz, S. W. *Prog. Photovoltaics: Res. Appl.* **2007**, *15*, 621.
(56) Chrisey, D. B.; Pique, A.; Modi, R.; Wu, H. D.; Auyeung, R. C. Y.; Young, H. D. *Appl. Surf. Sci.* **2000**, *168*, 345.
(57) Huang, J.; Kim, F.; Tao, A. R.; Connor, S.; Yang, P. *Nature Mater.* **2005**, *4*, 896.
(58) Tao, A. R.; Huang, J.; Yang, P. *Acc. Chem. Res.* **2008**, *41*, 1662.
(59) Zaumseil, J.; Meitl, M. A.; Hsu, J. W. P.; Acharya, B. R.; Baldwin, K. W.; Loo, Y.-L.; Rogers, J. A. *Nano Lett.* **2003**, *3*, 1223.
(60) Gates, B. D.; Xu, Q.; Stewart, M.; Ryan, D.; Willson, C. G.; Whitesides, G. M. *Chem. Rev.* **2005**, *105*, 1171.
(61) Hung, S.-C.; Nafday, O. A.; Haaheim, J. R.; Ren, F.; Chi, G. C.; Pearton, S. J. *J. Phys. Chem. C* **2010**, *114*, 9672.
(62) Todorov, T.; Mitzi, D. B. *Eur. J. Inorg. Chem.* **2009**, *2010*, 17.
(63) Ishihara, H.; Nakagawa, S.; Mochizuki, N.; Ishida, M. U.S. Patent 5,910,336, 1999.
(64) Weng, S.; Cocivera, M. *J. Appl. Phys.* **1993**, *74*, 2046.

(65) Beck, M. E.; Cocivera, M. *Thin Solid Films* **1996**, *272*, 71.
(66) Oliveira, L.; Todorov, T.; Chassaing, E.; Lincot, D.; Carda, J.; Escribano, P. *Thin Solid Films* **2009**, *517*, 2272.
(67) Kaelin, M.; Rudmann, D.; Kurdesau, F.; Zogg, H.; Meyer, T.; Tiwari, A. N. *Thin Solid Films* **2005**, *480*−*481*, 486.
(68) Weil, B. D.; Connor, S. T.; Cui, Y. *J. Am. Chem. Soc.* **2010**, *132*, 6642.
(69) Mitzi, D. B. *J. Mater. Chem.* **2004**, *14*, 2355.
(70) Zouaghi, M. C.; Nasrallah, T. B.; Marsillac, S.; Bernëde, J. C.; Belgacem, S. *Thin Solid Films* **2001**, *382*, 39.
(71) Krunks, M.; Kijatkina, O.; Rebane, H.; Oja, I.; Mikli, V.; Mere, A. *Thin Solid Films* **2002**, *403*−*404*, 71.
(72) Marsillac, S.; Zouaghi, M. C.; Bernëde, J. C.; Ben Nasrallah, T.; Belgacem, S. *Sol. Energy Mater. Sol. Cells* **2003**, *76*, 125.
(73) Li, L.; Coates, N.; Moses, D. *J. Am. Chem. Soc.* **2010**, *132*, 22.
(74) Kanatzidis, M. G.; Huang, S.-P. *Coord. Chem. Rev.* **1994**, *130*, 509.
(75) Banger, K. K.; Hollingsworth, J. A.; Harris, J. D.; Cowen, J.; Buhro, W. E.; Hepp, A. F. *Appl. Organomet. Chem.* **2002**, *16*, 617.
(76) Castro, S. L.; Bailey, S. G.; Raffaelle, R. P.; Banger, K. K.; Hepp, A. F. *Chem. Mater.* **2003**, *15*, 3142.
(77) Mitzi, D. B. *Adv. Mater.* **2009**, *21*, 3141.
(78) Yuan, M.; Mitzi, D. B. *Dalton Trans.* **2009**, 6078.
(79) Liu, W.; Mitzi, D. B.; Yuan, M.; Kellock, A. J.; Chey, S. J.; Gunawan, O. *Chem. Mater.* **2010**, *22*, 1010.
(80) Malik, J. A. N.; van Hest, M. F. A. M.; Miedaner, A.; Curtis, C. J.; Leisch, J. E.; Parilla, P. A.; Kaufman, M.; Taylor, M.; Stanbery, B. J.; O'Hhayre, R. P.; Ginley, D. S. *J. Mater. Res.* **2009**, *24*, 1375.
(81) Curtis, C. J.; Miendaner, A.; van Hest, M.; Ginley, D. S. WO Ppatent 063190, 2008.
(82) Mitzi, D. B.; Copel, M.; Chey, S. J. *Adv. Mater.* **2005**, *17*, 1285.
(83) Basol, B. L. M. *Thin Solid Films* **2000**, *361*−*362*, 514.
(84) Schulz, D.; Curtis, C.; Flitton, R.; Wiesner, H.; Keane, J.; Matson, R.; Jones, K.; Parilla, P.; Noufi, R.; Ginley, D. *J. Electron. Mater.* **1998**, *27*, 433.
(85) Guo, Q.; Kim, S. J.; Kar, M.; Shafarman, W. N.; Birkmire, R. W.; Stach, E. A.; Agrawal, R.; Hillhouse, H. W. *Nano Lett.* **2008**, *8*, 2982.
(86) Guo, Q.; Ford, G. M.; Hillhouse, H. W.; Agrawal, R. *Nano Lett.* **2009**, *9*, 3060.
(87) Panthani, M. G.; Akhavan, V.; Goodfellow, B.; Schmidtke, J. P.; Dunn, L.; Dodabalapur, A.; Barbara, P. F.; Korgel, B. A. *J. Am. Chem. Soc.* **2008**, *130*, 16770.
(88) Nanosolar, Inc. 17th International Photovoltaic Science and Engineering Conference, Tokyo, Japan, 2007.
(89) Bonnet, D. In *Clean Electricity from Photovoltaics*; Archer, M. D., Hill, R., Eds.; Imperial College Press: London, 2001.
(90) Miles, R. W.; Hynes, K. M.; Forbes, I. *Prog. Cryst. Growth Charact. Mater.* **2005**, *51*, 1.
(91) Miles, R. W. *Vacuum* **2006**, *80*, 1090.
(92) Cunningham, D. W.; Frederick, M.; Gittings, B.; Grammond, L.; Harrer, S.; Intagliata, J.; O'Cconnor, N.; Rubcich, M.; Skinner, D.; Veluchamy, P. Conference Record of the 29th IEEE Photovoltaic Specialists Conference, New Orleans, LA, 2002, p 559.
(93) Yoshida, T. *J. Electrochem. Soc.* **1995**, *142*, 3232.
(94) Schulz, D. L.; Pehnt, M.; Rose, D. H.; Urgiles, E.; Cahill, A. F.; Niles, D. W.; Jones, K. M.; Ellingson, R. J.; Curtis, C. J.; Ginley, D. S. *Chem. Mater.* **1997**, *9*, 889.
(95) Basol, B. M. *Int. J. Sol. Energy* **1992**, *12*, 25.
(96) Mccandless, B. E.; Moulton, L. V.; Birkmire, R. W. *Prog. Photovoltaics: Res. Appl.* **1997**, *5*, 249.
(97) Rose, D.; Powell, R.; Jayamaha, U.; Maltby, M.; Giolando, D.; Mcmaster, A.; Kormanyos, K.; Faykosh, G.; Klopping, J.; Dorer, G. Conference Record of the 28th IEEE Photovoltaic Specialists Conference, Anchorage, AK, 2000, p 428.
(98) Butler, D. *Nature* **2008**, *454*, 558.
(99) Feltrin, A.; Freundlich, A. *Renewable Energy* **2008**, *33*, 180.
(100) Ennaoui, A.; Fiechter, S.; Pettenkofer, C.; Alonso-Vante, N.; Büker, K.; Bronold, M.; Höpfner, C.; Tributsch, H. *Sol. Energy Mater. Sol. Cells* **1993**, *29*, 289.
(101) Dong, Y.; Zheng, Y.; Duan, H.; Sun, Y.; Chen, Y. *Mater. Lett.* **2005**, *59*, 2398.
(102) Gomes, A.; Ares, J.; Ferrer, I.; Da Silva Pereira, M.; Sanchez, C. *Mater. Res. Bull.* **2003**, *38*, 1123.
(103) Nakamura, S.; Yamamoto, A. *Sol. Energy Mater. Sol. Cells* **2001**, *65*, 79.
(104) Chatzitheodorou, G.; Fiechter, S.; Kunst, M.; Luck, J.; Tributsch, H. *Mater. Res. Bull.* **1988**, *23*, 1261.
(105) Smestad, G.; Da Silva, A.; Tributsch, H.; Fiechter, S.; Kunst, M.; Meziani, N.; Birkholz, M. *Sol. Energy Mater.* **1989**, *18*, 299.
(106) Birkholz, M.; Fiechter, S.; Hartmann, A.; Tributsch, H. *Phys. Rev. B* **1991**, *43*, 11926.
(107) Mishra, K.; Osseo-Asare, K. *J. Electrochem. Soc.* **1992**, *139*, 749.
(108) Boer, K. W. *J. Cryst. Growth* **1982**, *59*, 111.
(109) Stiddard, M. H. B. *J. Mater. Sci. Lett.* **1987**, *6*, 857.
(110) Hall, R. B.; Meakin, J. D. *Thin Solid Films* **1979**, *63*, 203.
(111) Mooney, J. B.; Radding, S. B. *Annu. Rev. Mater. Sci.* **2003**, *12*, 81.
(112) Levin, M. N.; Semenov, V. N.; Ostapenko, O. V. *Tech. Phys. Lett.* **2002**, *28*, 409.
(113) Rhee, J. H.; Lee, Y. H.; Bera, P.; Seok, S. I. *Chem. Phys. Lett.* **2009**, *477*, 345.
(114) Olsen, L. C.; Addis, F. W.; Miller, W. *Sol. Cells* **1982**, *7*, 247.
(115) Rai, B. P. *Sol. Cells* **1988**, *25*, 265.
(116) Han, K.; Tao, M. *Sol. Energy Mater. Sol. Cells* **2009**, *93*, 153.
(117) Katayama, J.; Ito, K.; Matsuoka, M.; Tamaki, J. *J. Appl. Electrochem.* **2004**, *34*, 687.
(118) Subramanian, B.; Sanjeeviraja, C.; Jayachandran, M. *Bull. Electrochem.* **2002**, *18*, 349.
(119) Mishra, K.; Rajeshwar, K.; Weiss, A.; Murley, M.; Engelken, R. D.; Slayton, M.; Mccloud, H. E. *J. Electrochem. Soc.* **1989**, *136*, 1915.
(120) Avellaneda, D.; Delgado, G.; Nair, M. T. S.; Nair, P. K. *Thin Solid Films* **2007**, *515*, 5771.
(121) Avellaneda, D.; Nair, M. T. S.; Nair, P. K. *Thin Solid Films* **2009**, *517*, 2500.
(122) Reddy, N. K.; Reddy, K. T. R. *Phys. B (Amsterdam)* **2005**, *368*, 25.
(123) Ito, K.; Nakazawa, T. *Jpn. J. Appl. Phys.* **1988**, *27*, 2094.
(124) Katagiri, H.; Jimbo, K.; Maw, W. S.; Oishi, K.; Yamazaki, M.; Araki, H.; Takeuchi, A. *Thin Solid Films* **2009**, *517*, 2455.
(125) Zoppi, G.; Forbes, I.; Miles, R. W.; Dale, P. J.; Scragg, J. J.; Peter, L. M. *Prog. Photovoltaics: Res. Appl.* **2009**, *17*, 315.
(126) Ennaoui, A.; Lux-Steiner, M.; Weber, A.; Abou-Ras, D.; Kötschau, I.; Schock, H.-W.; Schurr, R.; Hölzing, A.; Jost, S.; Hock, R.; Voss, T.; Schulze, J.; Kirbs, A. *Thin Solid Films* **2009**, *517*, 2511.
(127) Scragg, J. J.; Dale, P. J.; Peter, L. M. *Electrochem. Commun.* **2008**, *10*, 639.
(128) Moriya, K.; Watabe, J.; Tanaka, K.; Uchiki, H. *Phys. Status Solidi C* **2006**, *3*, 2848.
(129) Nakayama, N.; Ito, K. *Appl. Surf. Sci.* **1996**, *92*, 171.
(130) Kamoun, N.; Bouzouita, H.; Rezig, B. *Thin Solid Films* **2007**, *515*, 5949.
(131) Moritake, N.; Fukui, Y.; Oonuki, M.; Tanaka, K.; Uchiki, H. *Phys. Status Solidi C* **2009**, *6*, 1233.
(132) Steinhagen, C.; Panthani, M. G.; Akhavan, V.; Goodfellow, B.; Koo, B.; Korgel, B. A. *J. Am. Chem. Soc.* **2009**, *131*, 12554.
(133) Guo, Q.; Hillhouse, H. W.; Agrawal, R. *J. Am. Chem. Soc.* **2009**, *131*, 11672.
(134) Todorov, T.; Kita, M.; Carda, J.; Escribano, P. *Thin Solid Films* **2009**, *517*, 2541.
(135) Wronski, C. R.; Carlson, D. E. In *Clean Electricity from photovoltaics*; Archer, M. D., Hill, R., Eds.; Imperial College Press: London, 2001.
(136) Marschner, C.; Baumgartner, J.; Wallner, A. *Dalton Trans.* **2006**, 5667.
(137) Shimoda, T.; Matsuki, Y.; Furusawa, M.; Aoki, T.; Yudasaka, I.; Tanaka, H.; Iwasawa, H.; Wang, D.; Miyasaka, M.; Takeuchi, Y. *Nature* **2006**, *440*, 783.
(138) Furusawa, M.; Tanaka, H. In *Solution Processing of Inorganic Materials*; Mitzi, D. B., Ed.; John Wiley & Sons, Inc.: Hoboken, NJ, 2009.
(139) Han, S.; Dai, X.; Loy, P.; Lovaasen, J.; Huether, J.; Hoey, J. M.; Wagner, A.; Sandstrom, J.; Bunzow, D.; Swenson, O. F.; Akhatov, I. S.; Schulz, D. L. *J. Non-Cryst. Solids* **2008**, *354*, 2623.
(140) Kunze, K.; Haubrich, S.; Zurcher, F.; Ridley, B.; Rockenberger, J. U.S. Patent 7,553,545, 2009.
(141) Rogojina, E. V.; Jayaraman, M.; Vanheusden, K. U.S. Patent 7,727,901, 2010.
(142) Tanaka, H.; Iwasawa, H.; Wang, D.; Toyoda, N.; Aoki, T.; Yudasaka, I.; Matsuki, Y.; Shimoda, T.; Furusawa, M. *Jpn. J. Appl. Phys.* **2007**, *46*, L886.
(143) Chopra, K. L.; Paulson, P. D.; Dutta, V. *Prog. Photovoltaics: Res. Appl.* **2004**, *12*, 69.
(144) Kessler, J.; Velthaus, K. O.; Ruckh, M.; Laichinger, R.; Schock, H. W.; Lincot, D.; Ortega, R.; Vedel, J. Proceedings of the 6th International Photovoltaic Science and Engineering Conference, New Delhi, India, 1992, p 1005.
(145) Ramanarhan, K.; Wiesner, H.; Asher, S.; Niles, D.; Bhattacharya, R. N.; Keane, J.; Contreras, M. A.; Noufi, R. Proceedings of the 2nd World Conference on Photovoltaic Energy Conversion, Vienna, Austria, 1998, p 477.
(146) Schulmeyer, T.; Hunger, R.; Fritsche, R.; Jäckel, B.; Jaegermann, W.; Klein, A.; Kniese, R.; Powalla, M. *Thin Solid Films* **2005**, *480*−*481*, 110.
(147) Hariskos, D.; Spiering, S.; Powalla, M. *Thin Solid Films* **2005**, *480*−*481*, 99.
(148) Naghavi, N.; Abou-Ras, D.; Allsop, N.; Barreau, N.; Bücheler, S.; Ennaoui, A.; Fischer, C.-H.; Guillen, C.; Hariskos, D.; Herrero, J.; Klenk, R.; Kushiya, K.; Lincot, D.; Menner, R.; Nakada, T.; Platzer-

Björkman, C.; Spiering, S.; Tiwari, A. N.; Törndahl, T. *Prog. Photovoltaics: Res. Appl.* **2010**, *18*, 411.
(149) Wager, J. F.; Keszler, D. A.; Presley, R. E. *Transparent Electronics*; Springer: New York, 2008.
(150) Hosono, H. *Thin Solid Films* **2007**, *515*, 6000.
(151) Niesen, T. P.; De Guire, M. R. *J. Electroceram.* **2001**, *6*, 169.
(152) Oktik, S. *Prog. Cryst. Growth Charact.* **1988**, *17*, 171.
(153) Exarhos, G. J.; Zhou, X.-D. *Thin Solid Films* **2007**, *515*, 7025.
(154) Ozgur, U.; Alivov, Y. I.; Liu, C.; Teke, A.; Reshchikov, M. A.; Dogan, S.; Avrutin, V.; Cho, S. J.; Morkoc, H. *J. Appl. Phys.* **2005**, *98*, 041301.
(155) Meyers, S. T.; Anderson, J. T.; Hung, C. M.; Thompson, J.; Wager, J. F.; Keszler, D. A. *J. Am. Chem. Soc.* **2008**, *130*, 17603.
(156) Olson, D. C.; Lee, Y.-J.; White, M. S.; Kopidakis, N.; Shaheen, S. E.; Ginley, D. S.; Voigt, J. A.; Hsu, J. W. P. *J. Phys. Chem. C* **2008**, *112*, 9544.
(157) Shimono, D.; Tanaka, S.; Torikai, T.; Watari, T.; Murano, M. *J. Ceram. Process. Res.* **2001**, *2*, 184.
(158) Gledhill, S.; Grimm, A.; Allsop, N.; Koehler, T.; Camus, C.; Lux-Steiner, M.; Fischer, C.-H. *Thin Solid Films* **2009**, *517*, 2309.
(159) Chopra, K. L.; Major, S.; Pandya, D. K. *Thin Solid Films* **1983**, *102*, 1.
(160) Tahar, R. B. H.; Ban, T.; Ohya, Y.; Takahashi, Y. *J. Appl. Phys.* **1998**, *83*, 2631.
(161) Fortunato, E.; Ginley, D.; Hosono, H.; Paine, D. C. *MRS Bull.* **2007**, *32*, 242.
(162) Khan, A. F.; Mehmood, M.; Rana, A. M.; Bhatti, M. T. *Appl. Surf. Sci.* **2009**, *255*, 8562.
(163) Moholkar, A. V.; Pawar, S. M.; Rajpure, K. Y.; Bhosale, C. H.; Kim, J. H. *Appl. Surf. Sci.* **2009**, *255*, 9358.
(164) Joseph, D. P.; Renugambal, P.; Saravanan, M.; Raja, S. P.; Venkateswaran, C. *Thin Solid Films* **2009**, *517*, 6129.
(165) Jarzebski, Z. M.; Marton, J. P. *J. Electrochem. Soc.* **1976**, *123*, C199.
(166) Granqvist, C. G. *Sol. Energy Mater. Sol. Cells* **2007**, *91*, 1529.
(167) Niklasson, G. A.; Granqvist, C. G. *J. Mater. Chem.* **2007**, *17*, 127.
(168) Powell, R. J.; Spicer, W. E. *Phys. Rev. B* **1970**, *2*, 2182.
(169) Sato, H.; Minami, T.; Takata, S.; Yamada, T. *Thin Solid Films* **1993**, *236*, 27.
(170) Chesin, J. P.; Steirer, K. X.; Widjonarko, N. E.; Berry, J. J.; Miedaner, A.; Ginley, D. S.; Olson, D. C. *Org. Electron.* **2010**, *11*, 1414.
(171) Han, S. Y.; Lee, D. H.; Chang, Y. J.; Ryu, S. O.; Lee, T. J.; Chang, C. H. *J. Electrochem. Soc.* **2006**, *153*, C382.
(172) Berkat, L.; Cattin, L.; Reguig, A.; Regragui, M.; Bernëde, J. C. *Mater. Chem. Phys.* **2005**, *89*, 11.
(173) Joseph, D. P.; et al. *Nanotechnology* **2008**, *19*, 485707.
(174) Mahmoud, S. A.; Akl, A. A.; Kamal, H.; Abdel-Hady, K. *Phys. B (Amsterdam)* **2002**, *311*, 366.
(175) Reguig, B. A.; Khelil, A.; Cattin, L.; Morsli, M.; Bernëde, J. C. *Appl. Surf. Sci.* **2007**, *253*, 4330.
(176) Romero, R.; Martin, F.; Ramos-Barrado, J. R.; Leinen, D. *Thin Solid Films* **2010**, *518*, 4499.
(177) Desai, J. D.; Min, S.-K.; Jung, K.-D.; Joo, O.-S. *Appl. Surf. Sci.* **2006**, *253*, 1781.
(178) Kamal, H.; Elmaghraby, E. K.; Ali, S. A.; Abdel-Hady, K. *J. Cryst. Growth* **2004**, *262*, 424.
(179) Vidales-Hurtado, M. A.; Mendoza-Galván, A. *Mater. Chem. Phys.* **2008**, *107*, 33.
(180) Lee, Y.-M.; Lai, C.-H. *Solid-State Electron.* **2009**, *53*, 1116.
(181) Purushothaman, K. K.; Muralidharan, G. *J. Sol−Gel Sci. Technol.* **2008**, *46*, 190.
(182) He, Z.; Ji, Z.; Zhao, S.; Wang, C.; Liu, K.; Ye, Z. *Sol. Energy* **2006**, *80*, 226.
(183) Jiao, Z.; et al. *Nanotechnology* **2003**, *14*, 458.
(184) Park, Y. R.; Kim, K. J. *J. Cryst. Growth* **2003**, *258*, 380.
(185) Ait Aouaj, M.; Diaz, R.; Belayachi, A.; Rueda, F.; Abd-Lefdil, M. *Mater. Res. Bull.* **2009**, *44*, 1458.
(186) Ramaiah, K. S.; Raja, V. S.; Bhatnagar, A. K.; Tomlinson, R. D.; Pilkington, R. D.; Hill, A. E.; Chang, S. J.; Su, Y. K.; Juang, F. S. *Semicond. Sci. Technol.* **2000**, *15*, 676.
(187) Ogi, T.; Iskandar, F.; Itoh, Y.; Okuyama, K. *J. Nanopart. Res.* **2006**, *8*, 343.
(188) Verma, A.; Khan, F.; Kumar, D.; Kar, M.; Chakravarty, B. C.; Singh, S. N.; Husain, M. *Thin Solid Films* **2010**, *518*, 2649.
(189) Dghoughi, L.; Ouachtari, F.; Addou, M.; Elidrissi, B.; Erguig, H.; Rmili, A.; Bouaoud, A. *Phys. B (Amsterdam)* **2010**, *405*, 2277.
(190) Oshima, M.; Yoshino, K. *J. Electron. Mater.* **2010**, *39*, 819.
(191) Veluchamy, P.; Tsuji, M.; Nishio, T.; Aramoto, T.; Higuchi, H.; Kumazawa, S.; Shibutani, S.; Nakajima, J.; Arita, T.; Ohyama, H.; Hanafusa, A.; Hibino, T.; Omura, K. *Sol. Energy Mater. Sol. Cells* **2001**, *67*, 179.
(192) Hu, L.; Kim, H. S.; Lee, J.-Y.; Peumans, P.; Cui, Y. *ACS Nano* **2010**, *4*, 2955.
(193) Lee, J. Y.; Connor, S. T.; Cui, Y.; Peumans, P. *Nano Lett.* **2008**, *8*, 689.
(194) Lu, Y. C.; Chou, K. S. *Nanotechnology* **2010**, *21*, 215707.
(195) Lin, K.-M.; Chen, Y.-Y.; Chou, K.-Y. *J. Sol−Gel Sci. Technol.* **2009**, *49*, 238.
(196) Teng, K. F.; Vest, R. W. *IEEE Trans. Compon., Hybrids, Manuf. Technol.* **1987**, *10*, 545.
(197) Teng, K. F.; Vest, R. W. *IEEE Trans. Compon., Hybrids, Manuf. Technol.* **1988**, *11*, 291.
(198) Dearden, A. L.; Smith, P. J.; Shin, D.-Y.; Reis, N.; Derby, B.; O'Brien, P. *Macromol. Rapid Commun.* **2005**, *26*, 315.
(199) Junfeng, M.; Lovell, M. R.; Mickle, M. H. *IEEE Trans. Electron. Packag. Manuf.* **2005**, *28*, 265.
(200) Liu, Z.; Su, Y.; Varahramyan, K. *Thin Solid Films* **2005**, *478*, 275.
(201) Wu, J.-T.; Hsu, S. L.-C.; Tsai, M.-H.; Hwang, W.-S. *Thin Solid Films* **2009**, *517*, 5913.
(202) Wu, J.-T.; Hsu, S. L.-C.; Tsai, M.-H.; Hwang, W.-S. *J. Phys. Chem. C* **2010**, *114*, 4659.
(203) Wu, Y.; Li, Y.; Ong, B. S. *J. Am. Chem. Soc.* **2007**, *129*, 1862.
(204) Curtis, C. J.; Rivkin, T.; Miedaner, A.; Alleman, J.; Perkins, J.; Smith, L.; Ginley, D. S. *Mater. Res. Soc. Symp. Proc.* **2002**, *730*, 79.
(205) Hersh, P. A.; Curtis, C. J.; van Hest, M. F. A. M.; Kreuder, J. J.; Pasquarelli, R.; Miedaner, A.; Ginley, D. S. 2010, in preparation.
(206) Rivkin, T.; Curtis, C. J.; Miedaner, A.; Alleman, J.; Schulz, D. L.; Ginley, D. S. 198th Meeting of the Electrochemical Society, Phoenix, AZ, 2000.
(207) Rivkin, T.; Curtis., C. J.; Miedaner, A.; Perkins, J.; Alleman, J.; Ginley, D. S. Conference Record of the 29th IEEE Photovoltaic Specialists Conference, New Orleans, LA, 2002, p 1326.
(208) Schulz, D. L.; Curtis, C. J.; Ginley, D. S. U.S. Patent 6,830,778, 2004.
(209) van Hest, M. F. A. M.; Curtis, C. J.; Miedaner, A.; Pasquarelli, R. M.; Kaydanova, T.; Hersh, P.; Ginley, D. S. 33rd IEEE Photovoltaic Specialists Conference, San Diego, CA, 2008, p 1.
(210) van Hest, M. F. A. M.; Curtis, C. J.; Miedaner, A.; Pasquarelli, R. M.; Kreuder, J.; Hersh, P.; Ginley, D. S. 34th IEEE Photovoltaic Specialists Conference, Philadelphia, PA, 2009, p 1736.
(211) Jahn, S. F.; Blaudeck, T.; Baumann, R. R.; Jakob, A.; Ecorchard, P.; Rüffer, T.; Lang, H.; Schmidt, P. *Chem. Mater.* **2010**, *22*, 3067.
(212) Bidoki, S. M.; Lewis, D. M.; Clark, M.; Vakorov, A.; Millner, P. A.; Mcgorman, D. *J. Micromech. Microeng.* **2007**, *17*, 967.
(213) Li, D.; Sutton, D.; Burgess, A.; Graham, D.; Calvert, P. D. *J. Mater. Chem.* **2009**, *19*, 3719.
(214) Valeton, J. J. P.; Hermans, K.; Bastiaansen, C. W. M.; Broer, D. J.; Perelaer, J.; Schubert, U. S.; Crawford, G. P.; Smith, P. J. *J. Mater. Chem.* **2010**, *20*, 543.
(215) Perelaer, B. J.; Laat, A. W. M. D.; Hendriks, C. E.; Schubert, U. S. *J. Mater. Chem.* **2008**, *18*, 3209.
(216) Nir, M. M.; Zamir, D.; Haymov, I.; Ben-Asher, L.; Cohen, O.; Faulkner, B.; Vega, F. D. L. In *The Chemistry of Inkjet Inks*; Magdassi, S., Ed.; World Scientific Publishing Co. Pte. Ltd.: Hackensack, NJ, 2010.
(217) Liang, L. H.; Shen, C. M.; Du, S. X.; Liu, W. M.; Xie, X. C.; Gao, H. J. *Phys. Rev. B* **2004**, *70*, 205419.
(218) Lee, H.-H.; Chou, K.-S.; Huang, K.-C. *Nanotechnology* **2005**, *16*, 2436.
(219) Allen, M. L.; Aronniemi, M.; Mattila, T.; Alastalo, A.; Ojanperä, K.; Suhonen, M.; Seppä, H. *Nanotechnology* **2008**, *19*, 175201.
(220) Ko, S. H.; Pan, H.; Grigoropoulos, C. P.; Luscombe, C. K.; Frechet, J. M. J.; Poulikakos, D. *Appl. Phys. Lett.* **2007**, *90*, 141103.
(221) Yung, K.; Wu, S.; Liem, H. *J. Mater. Sci.* **2009**, *44*, 154.
(222) Perelaer, J.; De†Gans, B.-J.; Schubert, U. S. *Adv. Mater.* **2006**, *18*, 2101.
(223) Reinhold, I.; Hendriks, C. E.; Eckardt, R.; Kranenburg, J. M.; Perelaer, J.; Baumann, R. R.; Schubert, U. S. *J. Mater. Chem.* **2009**, *19*, 3384.
(224) Magdassi, S.; Grouchko, M.; Berezin, O.; Kamyshny, A. *ACS Nano* **2010**, *4*, 1943.
(225) Wakuda, D.; Keun-Soo, K.; Suganuma, K. *IEEE Trans. Compon. Packag. Technol.* **2009**, *32*, 627.
(226) Ginley, D. S. 195th Electrochemical Society Meeting, Seattle, WA, 1999, p 103.
(227) Tseng, W.; Chen, C.-N. *J. Mater. Sci.* **2006**, *41*, 1213.
(228) Schulz, D. L.; Curtis, C. J.; Ginley, D. S. *Electrochem. Solid-State Lett.* **2001**, *4*, C58.
(229) Schulz, D. L.; Ribelin, R.; Curtis, C. J.; Ginley, D. S. National Center for Photovoltaics (NCPV) 15th Program Review Meeting, Denver, CO, 1999, p 206.
(230) Curtis, C. J.; Miedaner, A.; Rivkin, T.; Alleman, J.; Schulz, D. L.; Ginley, D. S. *Mater. Res. Soc. Symp. Proc.* **2000**, *624*, 59.
(231) Jeong, S.; Woo, K.; Kim, D.; Lim, S.; Kim, J. S.; Shin, H.; Xia, Y.; Moon, J. *Adv. Funct. Mater.* **2008**, *18*, 679.
(232) Grouchko, M.; Kamyshny, A.; Magdassi, S. *J. Mater. Chem.* **2009**, *19*, 3057.

(233) Kim, S. J.; Stach, E. A.; Handwerker, C. A. *Appl. Phys. Lett.* **2010**, *96*, 144101.
(234) Woo, K.; Kim, D.; Kim, J. S.; Lim, S.; Moon, J. *Langmuir* **2009**, *25*, 429.
(235) Schubert, G.; Huster, F.; Fath, P. *Sol. Energy Mater. Sol. Cells* **2006**, *90*, 3399.
(236) Hong, K.-K.; Cho, S.-B.; You, J. S.; Jeong, J.-W.; Bea, S.-M.; Huh, J.-Y. *Sol. Energy Mater. Sol. Cells* **2009**, *93*, 898.
(237) Hörteis, M.; Gutberlet, T.; Reller, A.; Glunz, S. W. *Adv. Funct. Mater.* **2010**, *20*, 476.
(238) Mette, A.; Pysch, D.; Emanuel, G.; Erath, D.; Preu, R.; Glunz, S. W. *Prog. Photovoltaics: Res. Appl.* **2007**, *15*, 493.
(239) Kaydanova, T.; van Hest, M. F. A. M.; Miedaner, A.; Curtis, C. J.; Alleman, J. L.; Dabney, M. S.; Garnett, E.; Shaheen, S.; Smith, L.; Collins, R.; Hanoka, J. I.; Gabor, A. M.; Ginley, D. S. Conference Record of The 31st IEEE Photovoltaics Specialists Conference, Orlando, FL, 2005, p 1305.
(240) Hörteis, M.; Glunz, S. W. *Prog. Photovoltaics: Res. Appl.* **2008**, *16*, 555.
(241) Bähr, M.; Kim, S.; Sridharan, S.; Khadilkar, C.; Shaikh, A.; Köhler, I.; Reichardt, M.; Kumar, M. Proceedings of the 22nd European Photovoltaic Solar Energy Conference, Milan, Italy, 2007, p 1015.
(242) Green, M. A.; Basore, P. A.; Chang, N.; Clugston, D.; Egan, R.; Evans, R.; Hogg, D.; Jarnason, S.; Keevers, M.; Lasswell, P.; O'Sullivan, J.; Schubert, U.; Turner, A.; Wenham, S. R.; Young, T. *Sol. Energy* **2004**, *77*, 857.
(243) Lennon, A. J.; Utama, R. Y.; Lenio, M. A. T.; Ho-Baillie, A. W. Y.; Kuepper, N. B.; Wenham, S. R. *Sol. Energy Mater. Sol. Cells* **2008**, *92*, 1410.
(244) Lennon, A. J.; Ho-Baillie, A. W. Y.; Wenham, S. R. *Sol. Energy Mater. Sol. Cells* **2009**, *93*, 1865.

CR100191D